

UNCLASSIFIED

---

AD 275 459

*Reproduced  
by the*

ARMED SERVICES TECHNICAL INFORMATION AGENCY  
ARLINGTON HALL STATION  
ARLINGTON 12, VIRGINIA



---

UNCLASSIFIED

NOTICE: When government or other drawings, specifications or other data are used for any purpose other than in connection with a definitely related government procurement operation, the U. S. Government thereby incurs no responsibility, nor any obligation whatsoever; and the fact that the Government may have formulated, furnished, or in any way supplied the said drawings, specifications, or other data is not to be regarded by implication or otherwise as in any manner licensing the holder or any other person or corporation, or conveying any rights or permission to manufacture, use or sell any patented invention that may in any way be related thereto.

ARDD#2694:1

275 459

U. S. ARMY RESEARCH OFFICE (DURHAM)

Contract No. DA-11-022-ORD-3442

TECHNICAL REPORT NO. 7

APRIL 20, 1962

ELECTRICAL BEHAVIOR  
OF PASSIVE IRON (II)

By

J. L. ORD and J. H. BARTLETT

DEPARTMENT OF PHYSICS

UNIVERSITY OF ILLINOIS

Urbana, Illinois

ELECTRICAL BEHAVIOR OF PASSIVE IRON (II)

by

J. L. Ord and J. H. Bartlett

TECHNICAL REPORT NO. 7

Prepared under Contract No. DA-11-022-ORD-3442  
with the U. S. Army Research Office (Durham) for

PROTECTION AGAINST CORROSION

D/A Project No. 5B-01-004

ORD Project TB-2-001

OOR Project 2694-C

J. H. Bartlett, Technical Supervisor

University of Illinois, Urbana, Illinois

Requests for additional copies by Agencies of the Department of Defense, their contractors, and other Government agencies should be directed to Armed Services Technical Information Agency, Arlington Hall Station, Arlington 12, Virginia. Department of Defense contractors must be established for ASTIA services or have their "need-to-know" certified by the cognizant military agency of their project or contract.

All other persons and organizations should apply to the U. S. Department of Commerce, Office of Technical Services, Washington 25, D. C.

April 1962

## ABSTRACT

The electrical behavior of a passive iron electrode has been studied in an attempt to resolve the conflict between the layer and adsorption theories of passivity. A quantitative study of the dependence of current on potential has been made using steady-state, transient, and a-c measurements.

The steady-state current is independent of potential over most of the passive region. Transient measurements show that current depends exponentially on potential, and they establish capacitance as a parameter of the system. The parameters of the exponential dependence are determined by analyzing the shape of capacitive transients. These parameters are studied as functions of the variables of the system: temperature, concentration, steady-state potential, and, in the case of transients starting from other than steady states, current.

The physical significance of these parameters is interpreted in terms of a model incorporating a variable thickness surface layer and an interfacial current-limiting activation barrier. The parameters measured experimentally determine the parameters of the layer and the activation barrier. The layer varies from a minimum thickness of 12 Å at low overpotentials to a thickness of just over 100 Å before oxygen evolution begins. The height of the barrier is 1.58 eV and its jump distance is 2.81 Å. The calculation

of these numbers involves some assumptions which have not been checked experimentally, hence this model can only be taken as an order of magnitude model until further experimental information becomes available.

The overpotential parameters are found to have a significant current dependence. In its present state a space charge theory cannot account for the details of this dependence.

The kinetics of formation and removal of the layer are studied, and it is found that for anodic currents the rate of change of layer thickness is proportional to the difference between the anodic current and the steady-state current. For cathodic currents the electrode is activated by another mechanism before significant change in thickness is observed.

Transient and a-c measurements of capacitance show a correlation, and hence the parameter is physically significant. A potential region is found over which the reciprocal capacitance is linearly dependent on potential. The capacitance does not vary inversely as the thickness of the layer, but a component of it may.

## TABLE OF CONTENTS

I.	INTRODUCTION.....	1
II.	EXPERIMENTAL.....	6
III.	THE STEADY STATE.....	14
IV.	THE OVERPOTENTIAL PARAMETERS.....	24
V.	THE PASSIVE STATE TO ACTIVE STATE TRANSITION..	39
VI.	KINETICS OF FORMATION AND REMOVAL OF THE PASSIVE LAYER.....	51
VII.	THE A-C IMPEDANCE.....	67
VIII.	DISCUSSION.....	76
IX.	SUMMARY.....	84
	REFERENCES.....	87

## I. INTRODUCTION

Passivity is a phenomenon which has been known for many years, but which still lacks an adequate explanation. Passivity can be defined with reference to the electrical behavior of a metal in a corrosive electrolyte. Fig. 1 shows a schematic current-potential characteristic typical of a passive metal. When the electrode is placed in the electrolyte it reacts and assumes the corrosion potential. If an external voltage source is connected to the cell, and the electrode potential is made anodic, the reaction accelerates and a large current flows. As the potential is made more anodic, the current rises to a maximum, then falls sharply and becomes independent of potential until it rises again as oxygen evolution commences. The shape of the current-potential characteristic provides a natural division of the anodic potential range into three regions. The high-current region just above the corrosion potential is known as the active region. The low current region above the active region is known as the passive region. Potentials more noble than passive potentials are in the oxygen evolution region. Currents in the passive region are typically four orders of magnitude smaller than currents in the active region, so the phenomenon is well defined and easily observed. The presence of a redox system in the electrolyte may mask this behavior, but using the theory of mixed potentials the current can be resolved into a component whose behavior



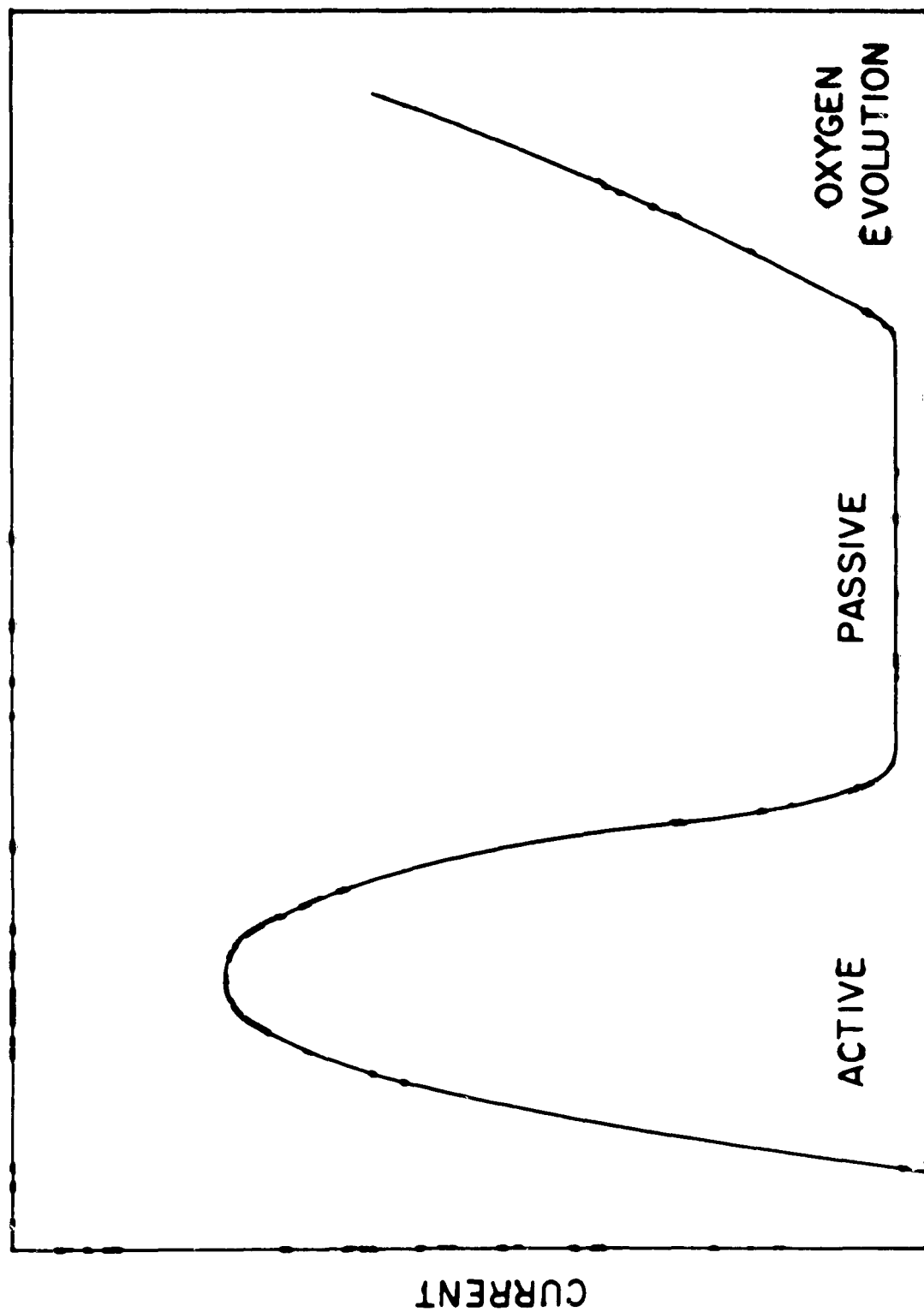


Fig. 1. Current-potential characteristic typical of passive metal (schematic).

resembles Fig. 1. Some metals, notably nickel, have a more complicated characteristic because the current shows a potential dependence in the passive region. The presence of the active state distinguishes passivity from anodic oxidation with which it has much in common.

Although experimental work has been carried out in the field for many decades, the explanation of passivity will have to await further experimental evidence. The First International Conference on Passivity helped to focus attention on the problem. The proceedings of the conference<sup>1/</sup> are doubly valuable: They present the state of knowledge of passivity as of September 1957, and through the references appended to the papers they provide access to the entire field. This single reference provides the bibliography for this work; all other references concern specific points.

Most of the experimental work has attempted to determine what "causes" passivity. There are two schools of thought on this question. One group believes that adsorption on the electrode surface inhibits the reaction and causes the very low currents observed. The other group believes that the low currents are due to the presence of a layer on the surface. The layer supporters believe that passivity is caused by a layer with a thickness of up to  $100 \text{ \AA}$ ; the adsorption supporters believe that passivity is caused by a monolayer or fraction thereof. The two schools of thought have come somewhat closer together in recent years, although their basic differences have become even more entrenched. This

paradoxical situation arises because the difference of opinion is concerned with the "cause" of passivity, not with what is present at the electrode-electrolyte interface. Adsorption theory explains a layer away as a reaction product incidental to passivity. Layer theory states that adsorption may be a step in the provision of oxygen for the formation of the layer.

It may be possible to determine experimentally that one or the other of the two theories is correct. On the other hand it may be impossible to fit the "cause" of passivity into either of these two categories. As an example of this consider Uhlig's experimental work<sup>2/</sup> on the connection between electron configuration in metals and passivity. He gives a reasonable interpretation of his results in terms of adsorption theory. It may be that adsorption is a necessary prerequisite to layer formation, but that it does not itself produce the low current characteristic of passivity, the low current being due to the ability of the layer to withstand a high electric field. If this turns out to be the case, it will be difficult to interpret the result as a victory for either side.

This work is not primarily concerned with the cause of passivity. It presents an attempt to study as completely as possible the electrical behavior of a passive iron electrode. The experimental results are partially correlated using a simple model of the passive electrode. An extension of this model may

lead to criteria for passivity, but the "cause" of passivity is not determined by this work.

The experimental program can be outlined briefly. First the current-potential characteristic is obtained from steady-state measurements. The dependence of current on potential is then investigated using transients, and the parameters of the dependence are determined. Transients are also used to determine the kinetics of formation and removal of the layer. Finally the a-c impedance of the passive electrode is studied to determine whether it is consistent with the transient measurements, or whether it provides additional information which must be correlated with the other measurements. The results are discussed in section VIII after all the measurements have been described. Some discussion is included as the results are presented in order to indicate the purpose of certain series of experiments.

## II. EXPERIMENTAL

The electrodes used in this investigation are prepared from high-purity iron obtained from several different sources. The highest quality material used is 99.99% pure 3/8" diameter rod supplied by A. D. MacKay, Inc. No significant difference in behavior is noted among electrodes prepared from different material. Electrodes made from sheet and wire material have been used, but the standard electrode used for most of the work is made from iron rod, and has a  $0.2 \text{ cm}^2$  nominal area single vertical face. This shape of electrode has the advantage that after deep etching it can be returned to its original nominal surface area by mechanical polishing. It has the disadvantage that there is a relatively long discontinuity between the electrode face and the coating compound. No ideal coating compound has been found although several compounds have been tried. Epoxy resin forms a transparent coating which permits detection of any leakage between the electrode and the coating compound, but mechanical polishing of this electrode tends to separate the epoxy resin from the iron rod. If the only effect of leakage were to increase the surface area it could be tolerated, but the electrode is not truly passive over the area where leakage occurs, and leakage currents are quite high. WD-4 shellac is used on most of the electrodes because it is easy to apply and forms an adherent coating.

The electrode surface is prepared by mechanical polishing through 4/0 emery paper followed by etching in the active state to remove the cold-worked layer and produce a stable surface area. Most electrodes exhibit a finely polycrystalline microstructure, and hence their surface becomes quite rough after etching. One anode with a larger grain size showed no difference in behavior except for a lower roughness factor. The electrode can be electropolished by holding it in the active state just below the potential at which it goes passive. In 2 N  $\text{H}_2\text{SO}_4$  a suitable polishing potential is -0.3 volts with respect to the sulphate electrode described below. A current of approximately  $200 \text{ ma/cm}^2$  flows during electropolishing and an opaque film covers the electrode surface.

A standard 250 ml beaker is used as a cell. During most experiments no attempt is made to exclude air from the cell. Experiments performed using nitrogen-saturated electrolyte give results identical with those obtained using air-saturated electrolyte. A sufficient partial pressure of hydrogen is maintained in the electrolyte to allow the platinized-platinum cathode to be operated as a reversible hydrogen electrode. Potentials are not measured with respect to the cathode, but it can be used as a check on potential measurements. A mercurous sulphate ( $.1 \text{ N K}_2\text{SO}_4 / \text{Hg}_2\text{SO}_4 / \text{Hg}$ ) electrode is used as a reference for potential measurement. This electrode is more suitable than the usual calomel

electrode because chlorine ions seriously contaminate the system. At room temperature in 2 N  $\text{H}_2\text{SO}_4$  the sulphate electrode has a potential of approximately +0.725 volts with respect to a reversible hydrogen electrode. Potentials are designated positive and negative in accordance with the international sign convention. All electrolytes are prepared from standard reagent grade chemicals. In some experiments the electrolyte is changed after passivation in order to remove the active-state reaction products, although no change in behavior is noted. 2 N  $\text{H}_2\text{SO}_4$  is used in all experiments except those explicitly studying the effects of acid concentration.

The circuitry used with the cell is shown schematically in Fig. 2. The circuit used to apply constant potential to the cell consists of a ten-turn 25-ohm Helipot in parallel with a bank of eighteen 2-volt Willard cells arranged to provide 2, 4, or 6 volts. The Thevenin equivalent resistance of this circuit is on the order of 10 ohms, and is not much greater than the resistance of the electrolyte (3 ohms). This type of potentiostat does not directly control the anode-reference potential, and thus it is important that the cathode be operated as a reversible hydrogen electrode. The galvanostat consists of a variable resistor in series with a 180-volt battery bank. The galvanostatic transients studied involve potential changes of less than 1 volt, and hence the galvanostat is accurate to better than 1%. A relay

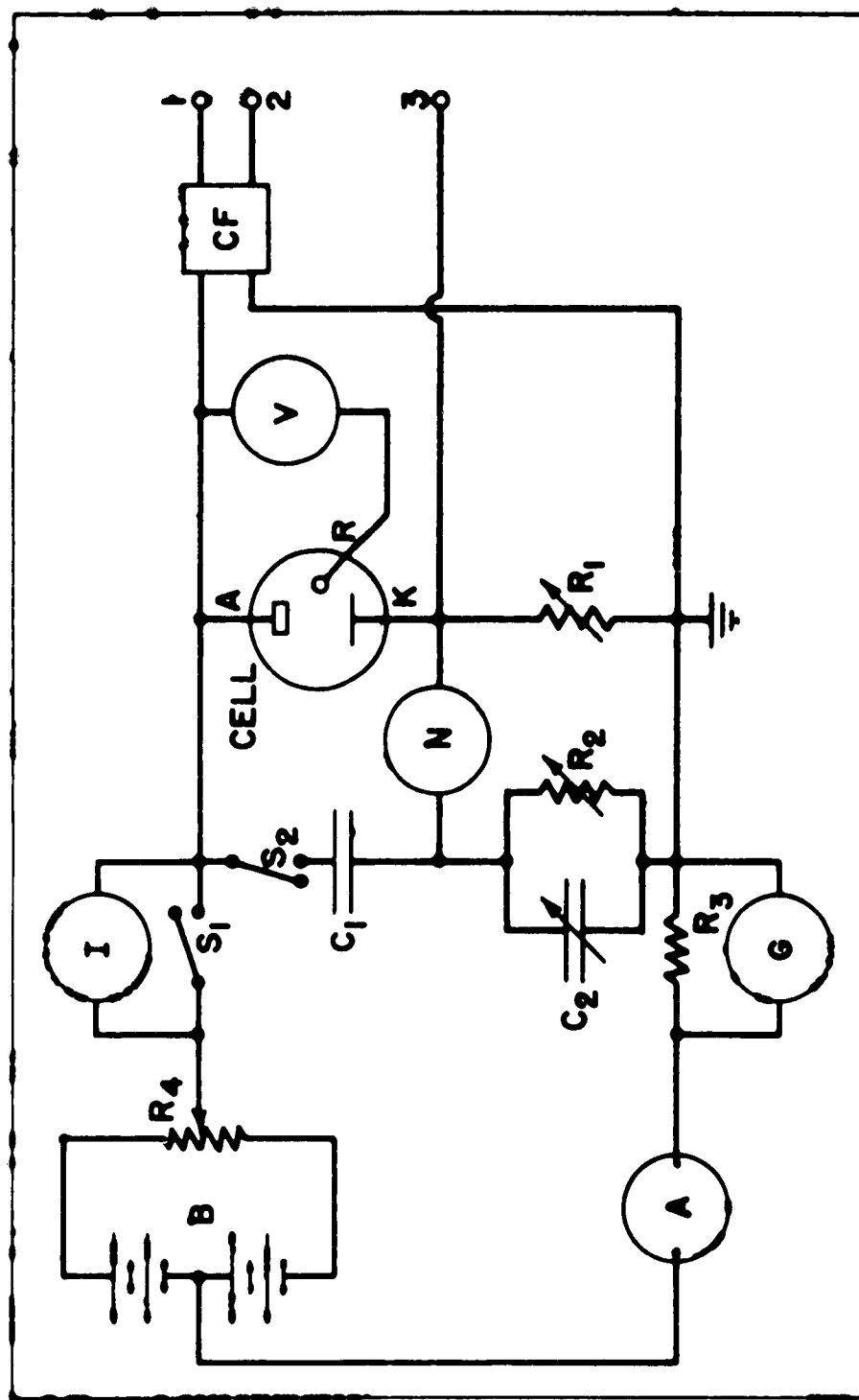


Fig. 2. Circuit diagram. A, anode; K, cathode; R, reference electrode; V, VTVM; CF, cathode follower; N, null detector; G, signal generator; I, constant current source; B, battery bank; A, microammeter.



bank consisting of three Westinghouse 375C relays is used to apply galvanostatic transients to the cell circuit. An RC circuit provides a calibrated delay of up to two seconds in the closing of one of the relays. Usually one relay is used to trigger the oscilloscope and the other two are used to apply the transient. The circuitry used to apply potentiostatic transients is not shown in the figure. In addition to the Helipot, fixed resistors can also be placed in parallel with the Willard cells. Potentiostatic transients are applied by using the relay bank to switch up or down across one of the fixed resistors. If current changes of less than 0.1 ma are studied the potential is constant to within 1 mv.

Potentials are read on the 1-volt scale of a Hewlett Packard 410A VTVM calibrated against a potentiometer. This instrument is convenient to use and has a high input impedance (100 megohms). Currents are usually large enough that they can be measured conveniently on a Weston 1306 microammeter (20 microamps full scale). A galvanometer is used to measure the smaller currents observed when higher pH electrolytes are used.

The usual method of recording data consists of photographing an oscilloscope trace. Three oscilloscopes are used: a Tektronix 512, a dual-beam Dumont 279, and an Analab 1100/700. A Praktica 35 mm single lens reflex camera and a 35 mm continuous motion camera are used in conjunction with the oscilloscopes. Data are analyzed using a microfilm reader.

The Analab oscilloscope is used for most of the work because it combines high gain (0.1 mv/cm) with widely variable sweep time (as slow as 5 sec/cm calibrated) and variable sweep length. This instrument has one drawback in this application: if a transient is spread over several sweeps to obtain optimum detail, an appreciable portion of the transient is lost between sweeps except at the slowest sweep times. The continuous motion camera can be used to avoid this problem. All of the oscilloscopes have too low an input impedance to permit potential transients to be observed directly. The d-c cathode follower circuit shown in Fig. 3 is used to provide high input impedance. The grid current of  $6 \times 10^{-9}$  amperes is smaller by almost three orders of magnitude than the steady-state current, and the 0.97 gain is high for a cathode follower. The cathode follower is battery operated because the biasing circuit tends to destroy the effect of feedback on the plate supply ripple. The capacitors are needed in the circuit to reduce stray pickup to an acceptable level. An electrometer has a much higher input impedance, but most electrometers have a narrow bandwidth and are not suitable for transient measurements.

The circuitry used to determine the a-c impedance of the cell is included in Fig. 2. A circuit of this type has the advantage that it is not necessary to isolate the a-c section. A Hewlett Packard 202B low frequency oscillator in parallel with a 5 ohm resistor is used for the a-c voltage source.

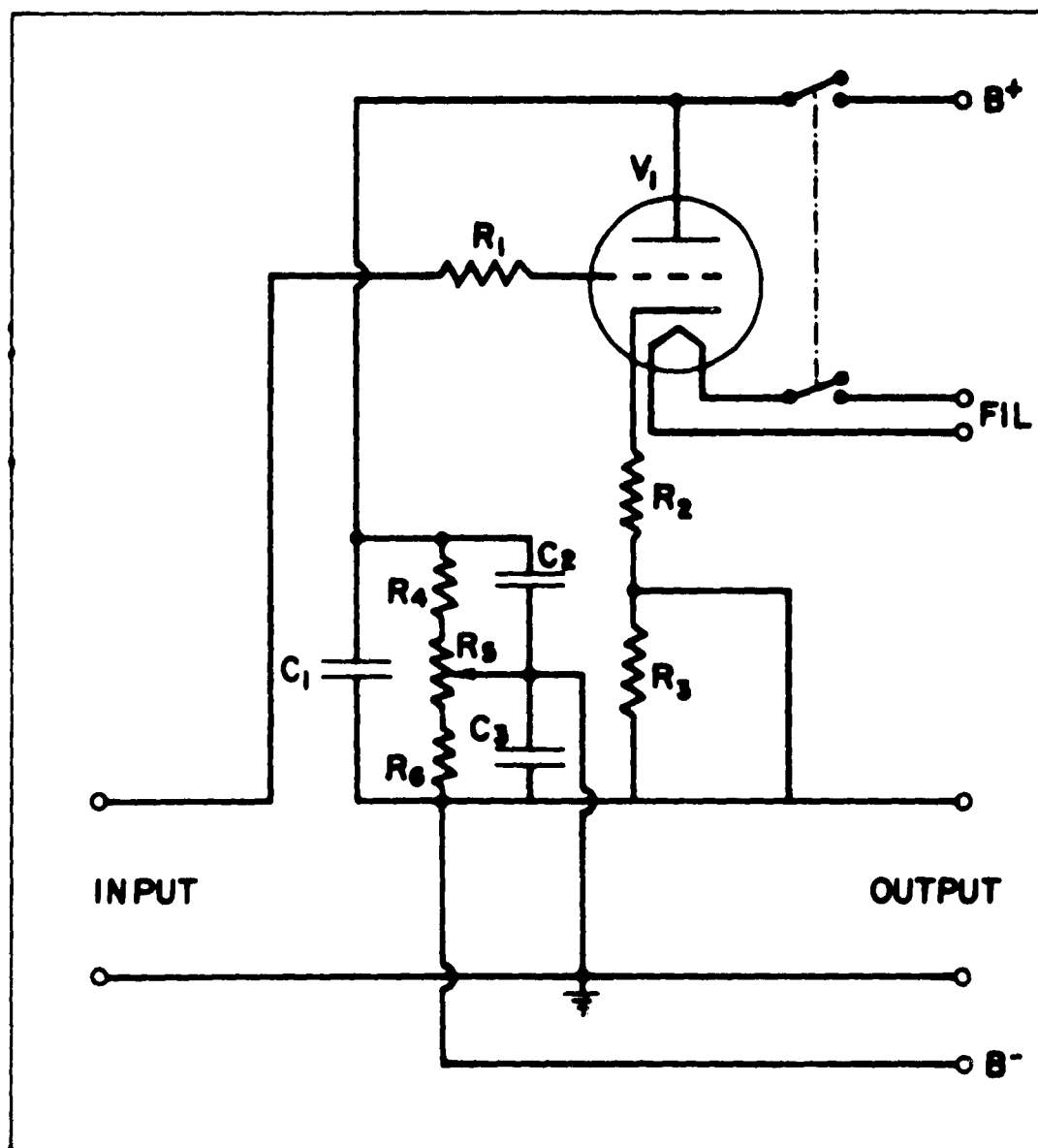


Fig. 5. Cathode follower circuit.  $V_1$ , 6F5;  $R_1$ , 22K;  
 $R_2$ , 2.5 K;  $R_3$ , 120 K;  $R_4$ , 100 K;  $R_5$ , 20 K;  $R_6$ ,  
 50 K;  $C_1$ , 1  $\mu$ f;  $C_2$ ,  $C_3$ , .5  $\mu$ f; B, 180 volts;  
 Fil. 6 volts (d-c).

The low resistance a-c and d-c voltage sources are placed in series across the cell and hence do not seriously interact.  $R_1$ ,  $R_2$ ,  $C_1$ , and  $C_2$  along with the cell make up a Schering a-c impedance bridge.  $R_1$  appears in series with the cell and is much smaller than the d-c resistance of the cell. The parallel branch consisting of  $C_1$ ,  $C_2$ , and  $R_2$  has infinite d-c impedance, and hence does not affect the d-c cell current. A high-gain null detector allows the bridge to be operated with 10 mv a-c across the cell. The balance equations for the Schering bridge, written in terms of an equivalent series resistance and capacitance for the cell impedance, are:

$$C_s = \frac{C_1 R_2}{R_1} \quad (1)$$

$$R_s = \frac{R_1 C_2}{C_1} \quad (2)$$

The a-c impedance can also be measured using only the variable precision resistor  $R_1$ . The magnitude of the impedance is obtained by comparing the magnitudes of the signals across the cell and  $R_1$ . The phase angle is read directly using the null-readout dial on the time axis of the Analab oscilloscope. This technique has been adapted by other workers<sup>3/</sup> for use during transients. The impedance bridge is more convenient for most measurements, but it is not suitable for use with transients.

### III. THE STEADY STATE

The steady-state current-potential characteristic of a passive iron anode in 2 N  $\text{H}_2\text{SO}_4$  is presented in Fig. 4. Only the passive region is shown in the figure; the active-state corrosion potential is located at -1.03 volts on the sulphate reference potential scale. Bartlett and Stephenson<sup>4/</sup> studied the active state and obtained the complete anodic current-potential characteristics of an iron electrode, but they did not measure the steady-state current (except for order of magnitude) in the passive region.

The points plotted in Fig. 4 are calculated from current readings taken thirty minutes after the anode is passivated. Potentiostatic measurements taken over a ten hour period show that after thirty minutes the current shows no further time dependence. The term "steady state" is used here to mean that the potential and current are independent of time, and is not intended to imply that all parameters are time-independent. Franck and Weil<sup>5/</sup> report much longer times for the electrode to reach a steady state, hence some comments on the technique used to passivate the electrode are in order.

If, during electropolishing, the potential is raised into the passive region, the electrode becomes passive with the opaque film intact. When the electrode is passivated in this manner a considerably longer time is required to reach a steady state. This problem is avoided by reversing the current and evolving hydrogen at the iron electrode immediately prior

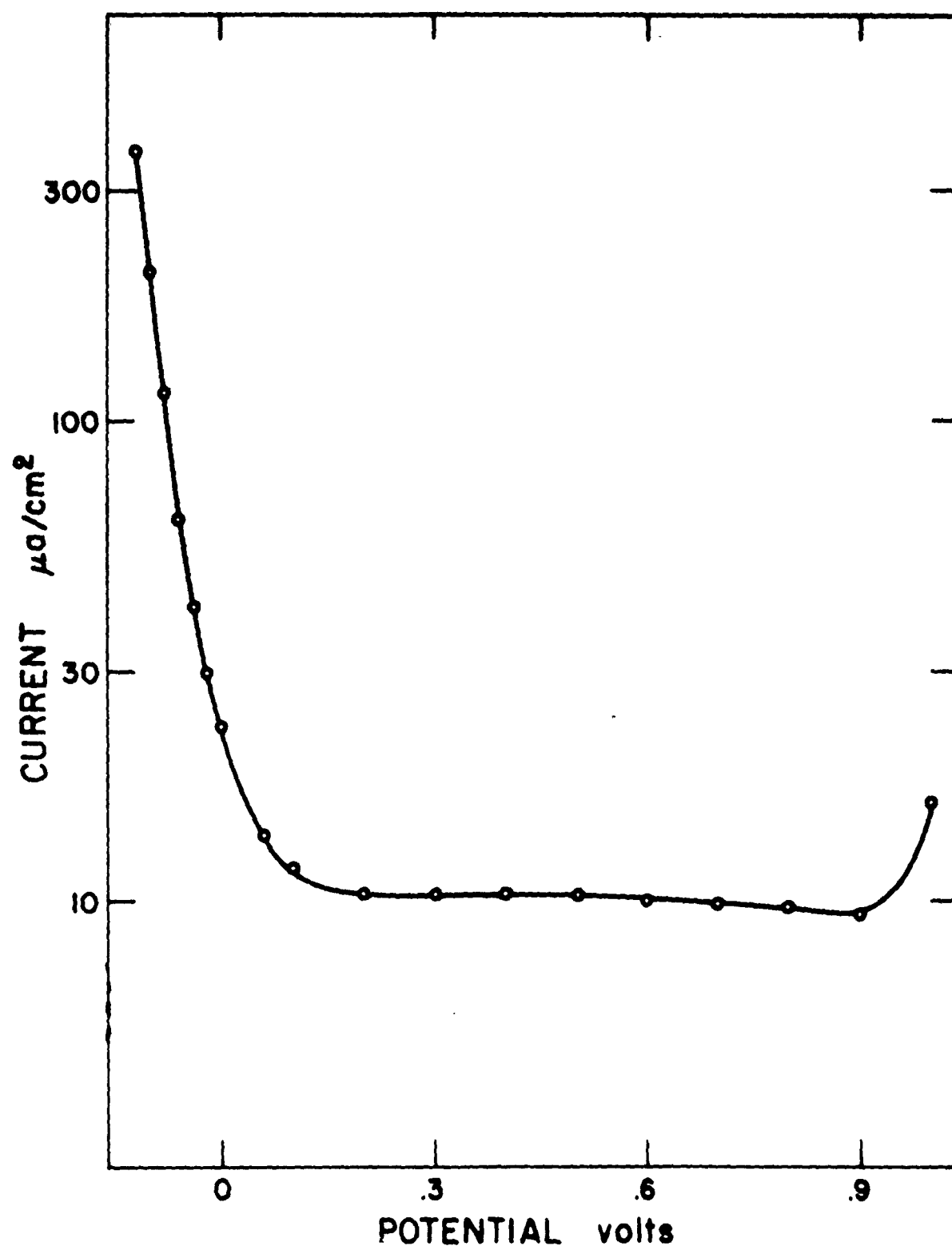


Fig. 4. Steady-state current versus potential.

to passivation. This can be accomplished by placing a switch between  $R_4$  and the positive end of the battery bank in Fig. 2. Electropolishing is interrupted by opening the switch;  $R_4$  is reset to give the required potential in the passive region; the switch is then reclosed. The electrode becomes passive within a few seconds of the reclosing of the switch. The surface of an electrode passivated in this manner appears perfectly clean to the naked eye, and a steady state is reached in about thirty minutes.

Franck and Weil passivate using constant current. The transition in this case is not from the active state to the passive state, but rather from the active state to oxygen evolution. The passive state is then reached by switching down to a constant potential in the passive region. Although a quantitative discussion of the dependence of the time required to reach a steady state upon the technique used for passivation must be postponed until the evidence for the existence of a variable thickness layer on the anode surface has been presented, some comments can be made at this point. A long time constant (i.e., greater than one hour) is not inherent in the active to passive transition. An intermediate step involving evolution of oxygen introduced into the active to passive transition results in a longer time being required to reach a steady state.

Fig. 4 can also be obtained by passivating the electrode and then observing the current as the potential is varied

over the passive region. Care must be taken to allow sufficient time for the electrode to reach a steady state at each potential, for otherwise a marked hysteresis is observed. when  $V$  is switched to a new value  $V + \Delta V$  we get a change of current  $\Delta i_1$ . If we now wait until the system settles to the steady state and then switch back suddenly to the original  $V$ , the current change will be much smaller than  $\Delta i_1$ , if  $\Delta V$  is sufficiently large. The time to recover to the steady state is now much longer than at the higher potential, because of the smaller current.

Over most of the passive region the steady-state current is independent of potential. Potentiostatic measurements are necessary to map out the curve in this region. At potentials above one volt the current rises rapidly and oxygen evolution is observed. In this region (which is not studied here) galvanostatic measurements are more suitable because of the steepness of the slope of the current-potential characteristic. At the negative end of the passive region the current also rises steeply. Although the steady-state characteristic behaves as a negative resistance in this region, the transient behavior is that of a positive resistance, and galvanostatic measurements are not possible. Under galvanostatic conditions any small fluctuation in potential will send the anode either across the passive region to oxygen evolution or into the active state. Stability in the negative resistance region is only possible if the external circuit has a load line with a



slope which is steeper than that of the steady-state current-potential characteristic. Since the current rises almost exponentially with decreasing potential in this region, stability eventually becomes a problem with even the best potentiostat. The impedance of the meter used to read the current limits stability with the equipment used here.

The steady-state current density in the potential-independent region is normalized to  $10 \mu\text{a}/\text{cm}^2$  at  $22^\circ \text{C}$ . This value represents a lower limit on the current density (referred to geometrical surface area), and can be attained only with very smooth electrodes. The etched electrodes which are used for most measurements have steady-state current densities which may be as high as  $20 \mu\text{a}/\text{cm}^2$ . It is assumed that variations in current density can be attributed to changes in roughness factor because capacitance, the other area-dependent parameter, shows the same dependence upon electrode surface treatment as does the current density. Franck and Weil<sup>5/</sup> find a steady-state current density of  $7 \mu\text{a}/\text{cm}^2$  for a passive iron anode in  $\text{N H}_2\text{SO}_4$  at  $25^\circ \text{C}$ . This value is in reasonable agreement with the one obtained here. A better parameter to use for comparison, and one which is independent of area, is the ratio of current to capacitance. The value for the capacitance obtained by Franck and Weil ( $63 \mu\text{f}/\text{cm}^2$ ) is higher by at least a factor of two than that obtained here and by other workers,<sup>6/</sup> and is apparently incorrect.

The dependence of the steady-state current upon the concentration of the sulphuric acid is shown in Fig. 5. To maintain high conductivity, the electrolytes in which the sulphuric acid concentration is below one normal have potassium sulphate added to maintain a one normal concentration of acid plus sulphate. For example the electrolyte plotted in the figure as .01 N  $\text{H}_2\text{SO}_4$  is actually .01 N  $\text{H}_2\text{SO}_4$  + .99 N  $\text{K}_2\text{SO}_4$ . These electrolytes have been used by other workers,<sup>7/</sup> and their pH is known.

Table 1. pH of electrolytes

Electrolyte	pH
1 N $\text{H}_2\text{SO}_4$	0.3
0.1 N $\text{H}_2\text{SO}_4$ + 0.9 N $\text{K}_2\text{SO}_4$	1.9
0.01 N $\text{H}_2\text{SO}_4$ + 0.99 N $\text{K}_2\text{SO}_4$	3.0

The dependence of the steady-state current upon temperature is presented in Fig. 6. The temperature range available for study is not very wide when compared to the absolute temperature, and hence the dependence cannot be uniquely determined from the data in Fig. 6 alone. It appears that the temperature dependence can be expressed as  $\exp(f(T))$  where  $f(T)$  is some function of the absolute temperature. The data can be fitted equally well to  $\alpha T$  or  $-\beta/T$  functions. If the process is activation controlled, the temperature

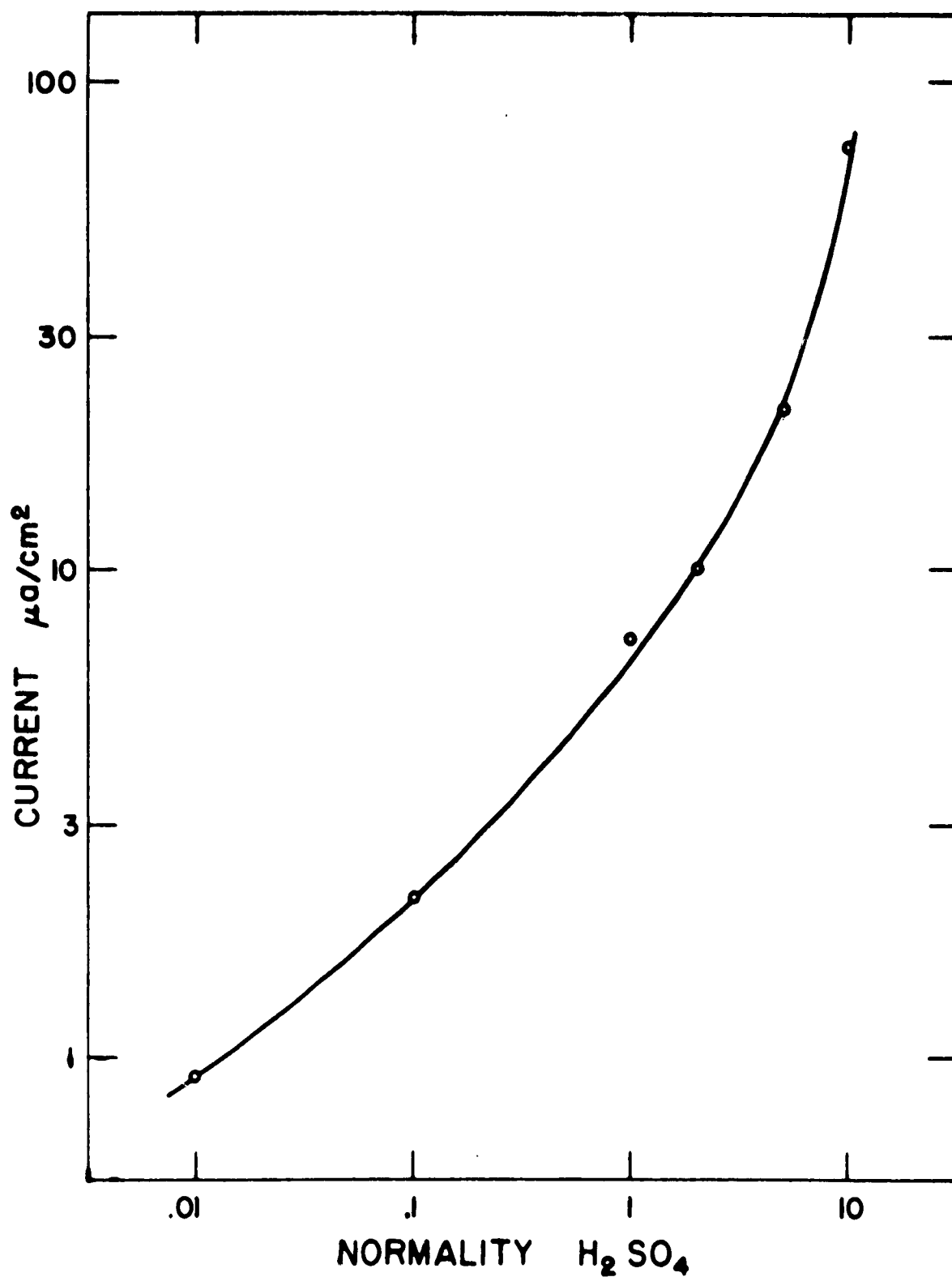


Fig. 4. Steady-state current versus normality  $\text{H}_2\text{SO}_4$ .  
Electrolytes less than 1 N in  $\text{H}_2\text{SO}_4$  have  $\text{H}_2\text{SO}_4$   
added to maintain 1 N total concentration.

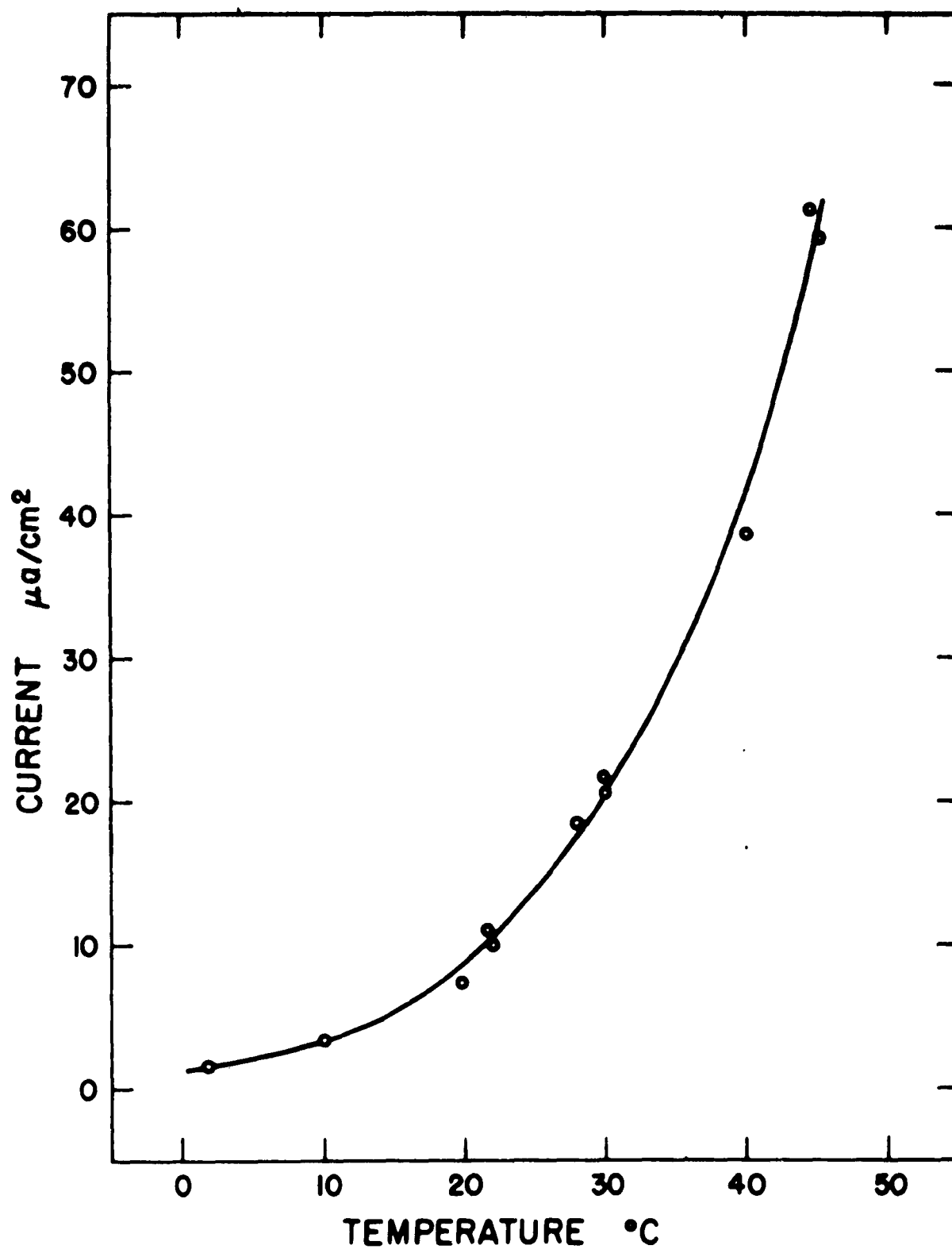


Fig. 6. Steady-state current versus temperature.

dependence should take the form  $\exp(-U/kT)$ , where  $U$  is the activation energy and  $k$  is Boltzmann's constant. Fig. 7 shows a plot of log current versus  $1/T$ . The straight line, fitted by least squares, gives an activation energy of 1.58 ev.

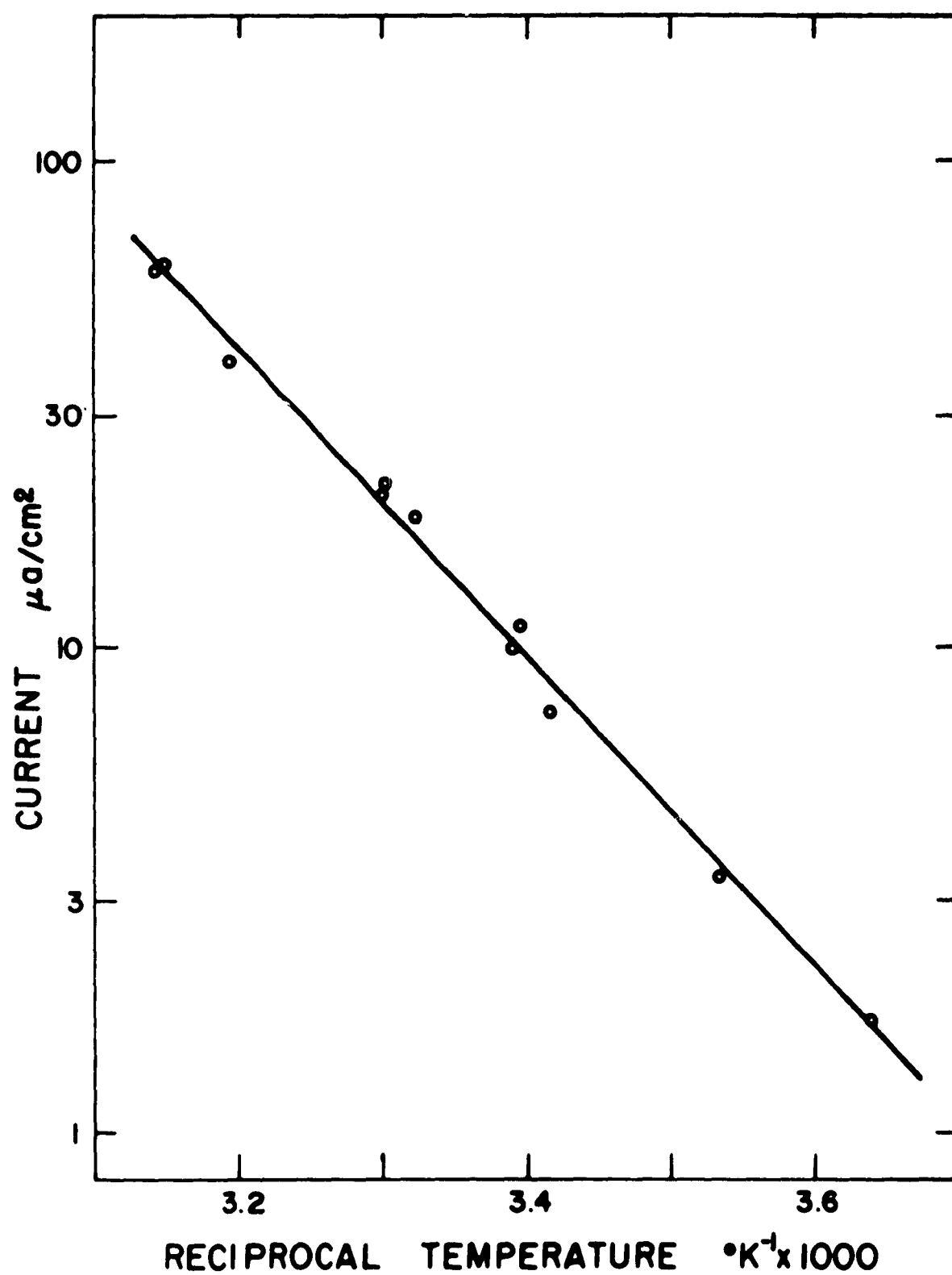


Fig. 7. Logarithm of steady-state current versus reciprocal temperature. Activation energy 1.58 ev.

#### IV. THE OVERPOTENTIAL PARAMETERS

Fig. 4 shows the dependence of current on potential when the electrode is in a steady state. It contains no information on how the current responds to changes in potential. In this chapter the dependence of current on potential is studied using transient measurements. The steady-state potential from which the transient is initiated is taken as a parameter in this dependence.

The steady-state measurements are performed at constant potential; potentiostatic transient measurements can be performed also. The potential is switched from one constant value to another and the current is recorded as a function of time. The resulting current transient has an initial spike which is limited only by the electrolyte resistance and the resistance of the external circuitry. The spike in the current indicates that capacitance is an important parameter in the system. Transients involving discontinuities in potential produce singularities in the current transient which greatly complicate analysis. This type of transient has been used by other workers,<sup>8/</sup> but the interpretation of the results is open to question.

Potential transients with no discontinuities can be produced by switching the current from one constant value to another. One such galvanostatic potential transient can be obtained simply by opening the circuit. A typical open-circuit transient starting from a steady state is shown

in Fig. 8. The transient is spread over several sweeps of the oscilloscope to bring out the shape of the curve in detail, and the figure is a copy of the photographed oscilloscope trace. The initial rapid potential decay is followed by a long sloping plateau followed in turn by a sharp transition to the corrosion potential. The plateau begins near the zero of the sulphate reference scale and extends down to approximately  $-.15$  volts. This is the potential range over which the current rises sharply as the potential decreases under steady-state conditions. Open-circuit transients which start from different potentials in the passive region are similar in shape, and have the plateau at approximately the same potential.

The initial part of Fig. 8 is similar in shape to the transient observed when a capacitor is discharged through a resistor. The component of potential which decays in this manner is called the overpotential. The term overpotential is used here to designate a potential which goes to zero as the current goes to zero. Since the plateau potential shows little dependence on the initial steady-state potential, the zero of overpotential is fixed, and the overpotential varies linearly with the passivating potential. The zero of overpotential can be defined as the extrapolation to zero time of the potential plateau. The definition actually used is taken from Fig 11 and is described later. It is not any better than the definition just given, but it is more convenient.



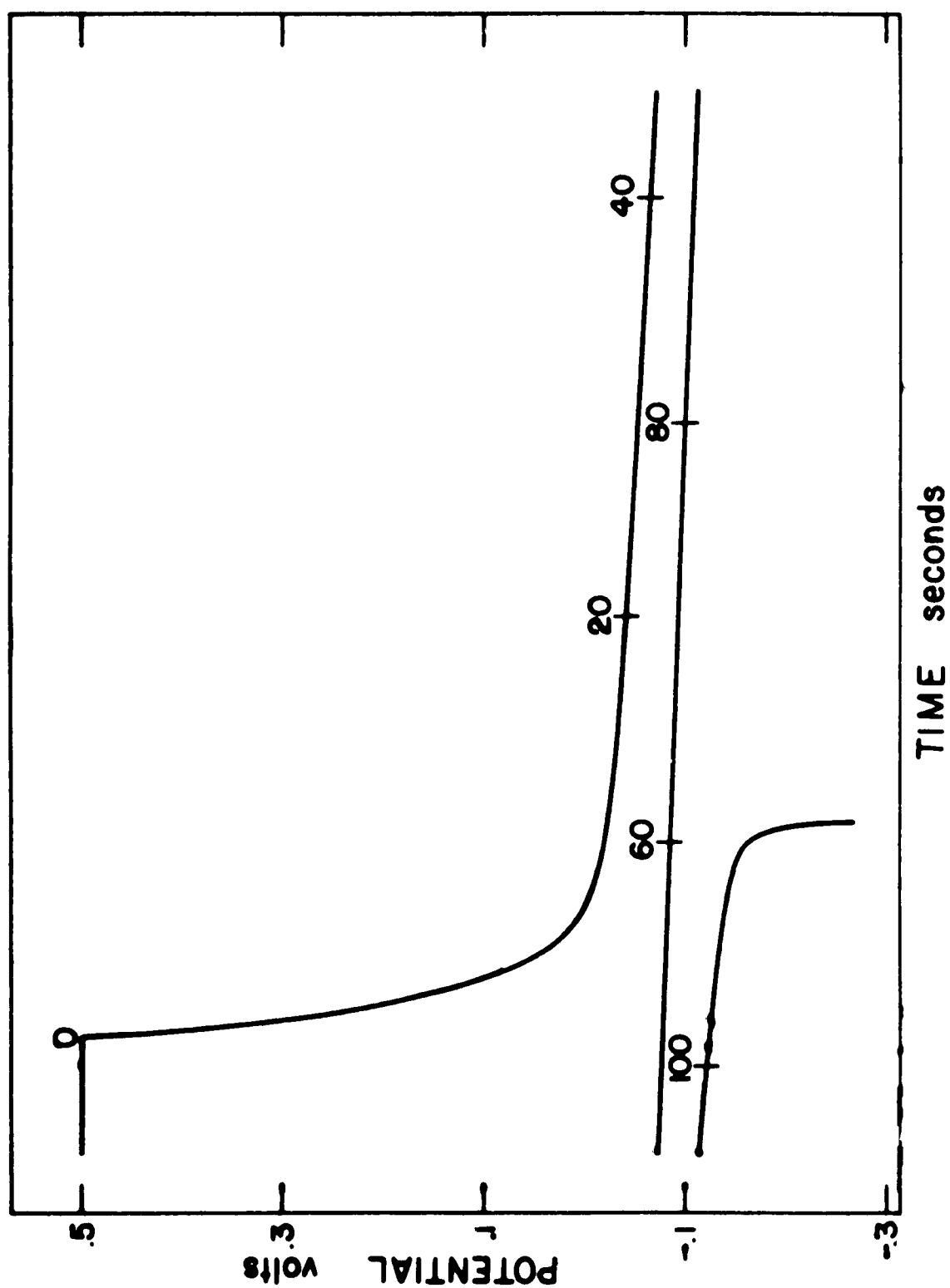


Fig. 8. Open-circuit potential transient. The corrosion potential (-1.03 volts) is not shown.

The dependence on potential of the current through the element in parallel with the capacitance can be determined by analyzing the shape of the capacitive transient. If the overpotential appears across a conducting medium, resistance,  $R$ , is the only parameter in the current-potential relation. The differential equation describing the circuit is:

$$i = C \, dv/dt + v/R \quad (3)$$

The solution for an open-circuit transient is:

$$v = v_i \exp(-t/RC) \quad (4)$$

where  $v_i$  is the initial potential. A plot of the transient on an exponential scale is shown in Fig. 9. The zero of overpotential is chosen to give the best fit to the experimental data. The points on the curve indicate the scatter in the data, not the number of points used for curve fitting. The initial portion of the curve cannot be made to fit a single exponential function. The initial deviation is compressed by the exponential scale; on a linear plot the transient requires quite a different shape to fit an exponential. This type of equivalent circuit can be generalized to include a number of  $R$   $C$  parallel elements arranged in series, and undoubtedly the transient can be fitted if sufficient elements are chosen. Some workers use this technique, but the physical significance of the parameters determined in this manner is questionable.

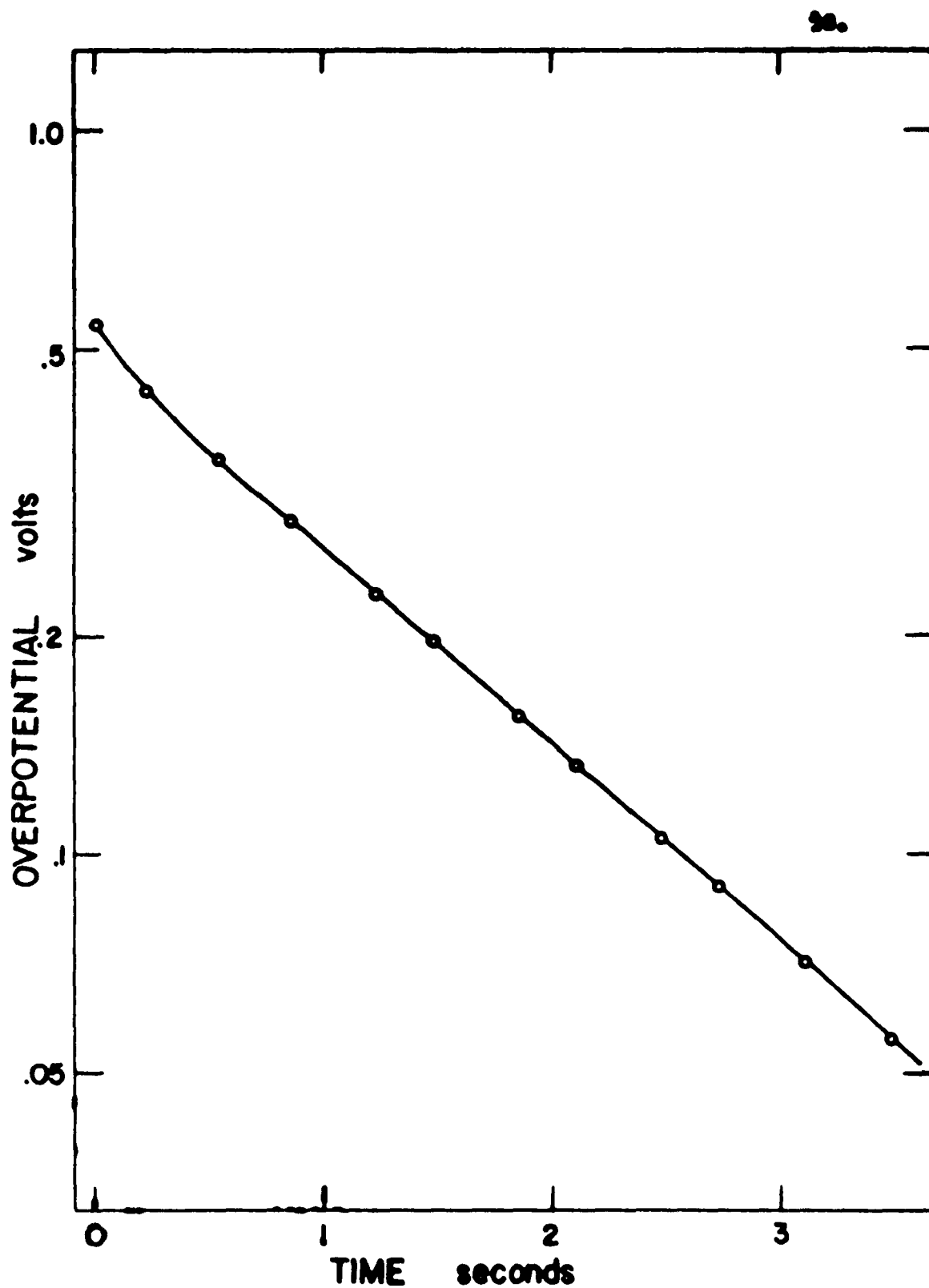


Fig. 9. Open-circuit potential transient with logarithmic potential scale. Zero of overpotential chosen for best fit to straight line.

If the overpotential appears across an activation barrier the relation between current and potential is more complicated. If the overpotential is high enough to make the reverse current across the barrier effectively zero, the total current is given by the forward current across the barrier. The forward current depends exponentially upon the energy of the charge carriers, and hence

$$i = i_0 \exp(v/v_0) \quad (5)$$

The parameters  $i_0$  and  $v_0$  are usually independent of current and potential, and they are taken as constants in the following equations. Eq. (5) has been derived by many authors,<sup>9/</sup> and the parameters have been expressed in terms of more fundamental electrochemical parameters. The differential equation describing this circuit is:

$$i = C \, dv/dt + i_0 \exp(v/v_0) \quad (6)$$

The circuit is non-linear and superposition is not valid. The solution of the differential equation for an open circuit transient is the only one which has a simple form:

$$\begin{aligned} i_0 \, dt &= - C \exp(-v/v_0) \, dv \\ i_0 (t + \theta) &= C v_0 \exp(-v/v_0) \\ v &= v_0 \ln(Cv_0/i_0) - v_0 \ln(t + \theta) \end{aligned} \quad (7)$$

To evaluate  $\theta$ , the constant of integration, use the boundary condition:

$$\text{at } t = 0, i = i_{ss} = i_o \exp(v_p/v_o)$$

$$v_p = v_o \ln(Cv_o/i_o\theta) \quad (8)$$

$$\theta = C v_o/i_o \exp(v_p/v_o) = C v_o/i_{ss}$$

The expression for the potential transient given in Eq. (7) will not be valid over the entire transient. Eq. (5) is only valid if the overpotential is sufficiently high to make the reverse current across the barrier effectively zero. As the overpotential decays it will eventually reach a value for which this condition does not hold.

Fig. 10 shows a logarithmic plot of an open-circuit transient. Again the points on the curve are only intended to indicate the scatter, not the number of points used for curve fitting. The curve is fitted by varying  $\theta$  until the curve becomes linear on the logarithmic scale. With an appropriate choice of  $\theta$  the fit is very good over the potential region where Eq. (5) can be expected to describe accurately the relation between current and potential. Some transients, notably those starting from higher potentials, have their initial points slightly above the line which fits the major portion of the curve. This deviation (a few millivolts) is not large enough to cast doubt upon the validity of an exponential relation between current and potential, but it is larger than the electrolyte  $iR$  drop. Three curves are presented in the figure to give some indication of the accuracy with which the parameters can be

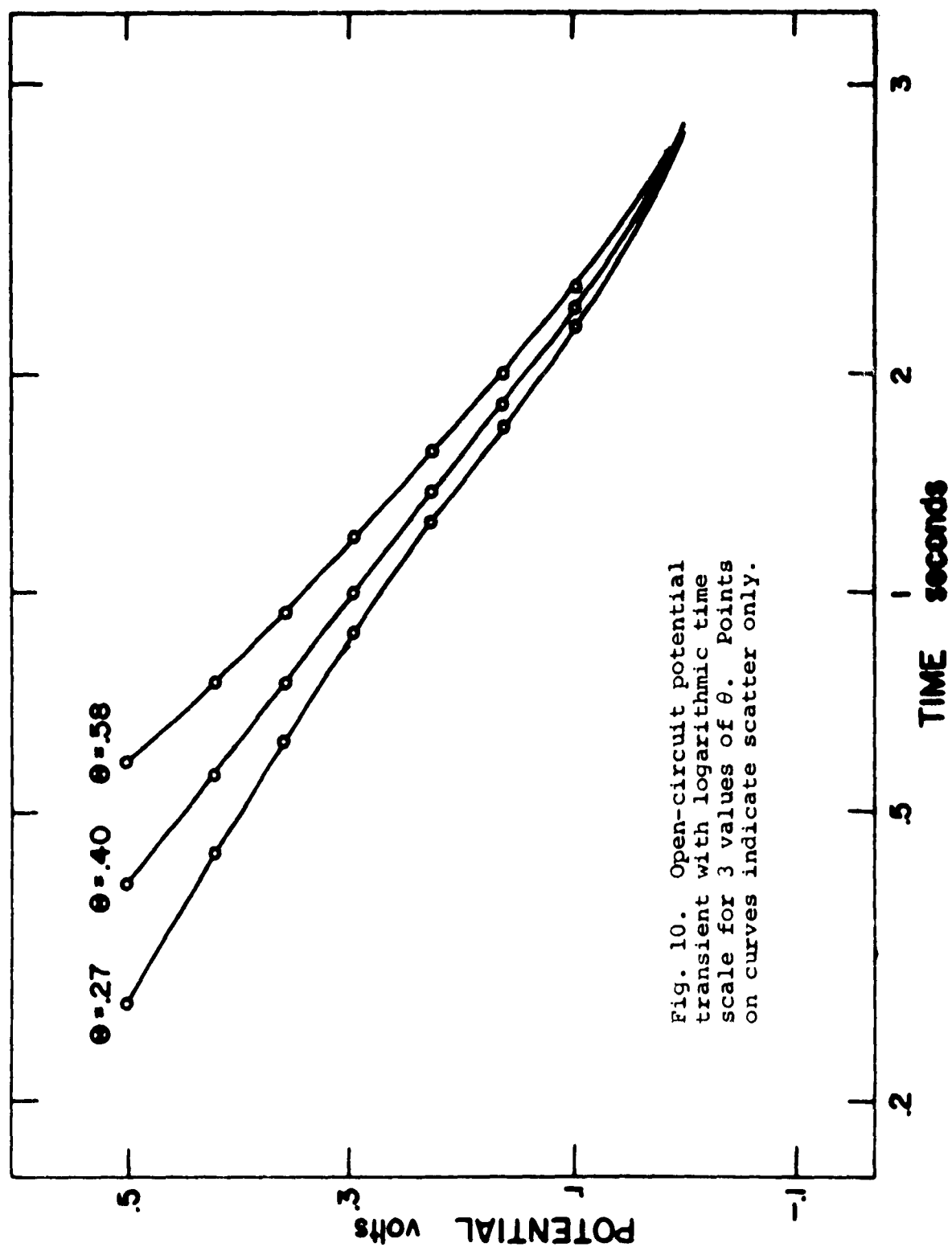


Fig. 10. Open-circuit potential transient with logarithmic time scale for 3 values of  $\theta$ . Points on curves indicate scatter only.

determined.  $\theta$  cannot be determined with very great accuracy, but  $v_o$  is not very sensitive to variations in  $\theta$ .  $i_o$  cannot be determined without information on the location of the zero of overpotential. Although the initial deviation is not large it has a significant effect on the initial slope of the transient. The capacitance can be determined either from the ratio of the initial current to the initial slope or from Eq. (8). Because of the initial deviation the two methods lead to different results.

A plot of  $v_o$  versus initial steady-state potential is given in Fig. 11. In the region where the steady-state current is constant,  $v_o$  rises linearly with potential at a slope of .386 (determined from a least squares fit). At lower potentials, where the current rises,  $v_o$  remains constant at .037 volts. The zero of overpotential used throughout this work is the intercept with the potential axis of the extrapolation of the plot as shown in Fig. 11. This definition is arbitrary, but it does agree well with the definition of the zero of overpotential obtained by extrapolating the open-circuit plateau back to zero time. This definition does have some advantages over the definition obtained from plateau extrapolation: the zero of overpotential and  $i_o$  are independent of the steady-state potential; the extrapolation of the  $v_o$  curve is straightforward and not subjective whereas the extrapolation of the plateau is difficult and liable to subjective error.

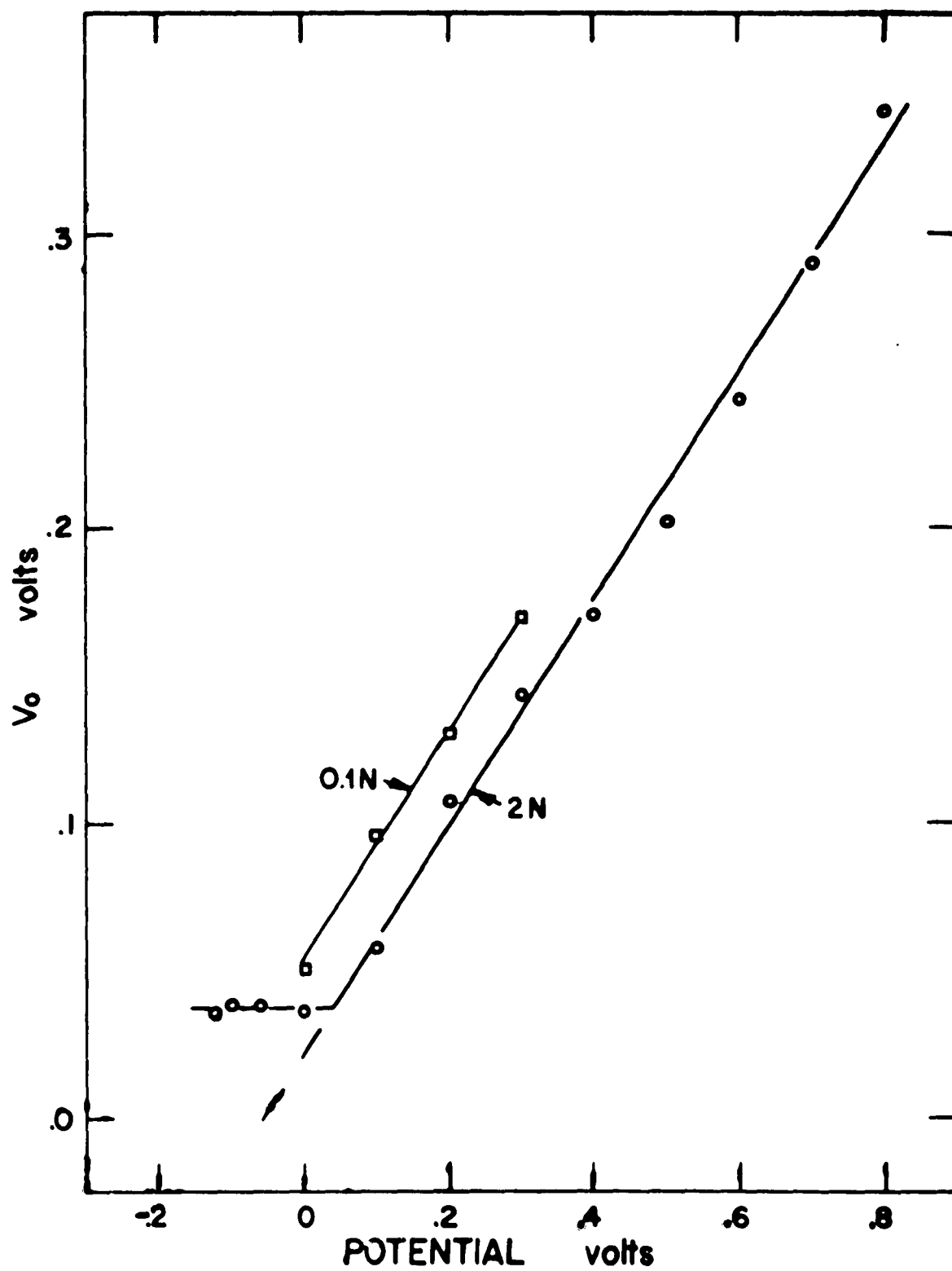


Fig. 11.  $v_o$  versus potential.



The zero of overpotential is taken to be  $-.055$  volts. This choice yields a value of  $.746 \mu\text{a}/\text{cm}^2$  for  $i_0$ .

A discussion of the physical significance of Fig. 11 is given in Section VIII. At this point a very brief discussion will be given in order to indicate the reason for carrying out the experiments described in Section VI. If the entire overpotential,  $v$ , appears across an activation barrier,  $v_0$  is constant. The curve in Fig. 11 is taken as an indication that the entire overpotential does not appear across an activation barrier. A simple model which accounts for the main features of Fig. 11 is obtained by assuming that a variable thickness layer is present at the electrode-electrolyte interface. The potential is assumed to vary linearly across the layer. At one interface of the layer there is an activation barrier which controls the current. The overpotential across this barrier is equal to the total overpotential multiplied by the ratio of the barrier jump distance to the layer thickness. With this model,  $v_0$  is proportional to the thickness of the layer. This model has been applied to the theory of oxidation by Cabrera and Mott.<sup>14/</sup> Many of the remaining experiments are designed to test this model and the assumption that  $v_0$  is a measure of the thickness of a layer present at the interface.

Before the capacitance can be determined a choice must be made between the initial slope data and the data obtained from Eq. (8). If Eq. (8) is used the initial deviation is

attributed to some element in series with the layer; if initial slopes are used the initial deviation must be attributed to a change in the parameters ( $i_o$ ,  $v_o$ , or both) of the element in parallel with the capacitance. The value of capacitance calculated from initial slope data is taken to be significant and is plotted versus passivating potential in Fig. 12. There are two reasons for this choice: the initial slopes of all galvanostatic transients give the same value for the capacitance independent of the current used, and the capacitance calculated from initial slopes can be correlated with the a-c capacitance measured in Section VII. It is assumed in what follows that the initial deviation is due to a rapid change in  $i_o$ , although this assumption is not essential. Reciprocal capacitance is plotted versus passivating potential in Fig. 13. The a-c values plotted in the same figure are taken from Fig. 33. Reciprocal capacitance is linearly dependent on but not proportional to overpotential. Capacitance shows some sign of the expected inverse dependence on thickness, but it must be influenced by other factors.

The concentration dependence of the overpotential parameters is determined by taking open-circuit transients in conjunction with the measurement of the dependence of the steady-state current upon concentration. A plot of  $v_o$  measured in 1 N  $H_2SO_4$  is included in Fig. 11. The shift between the two curves is due to the pH dependence of the

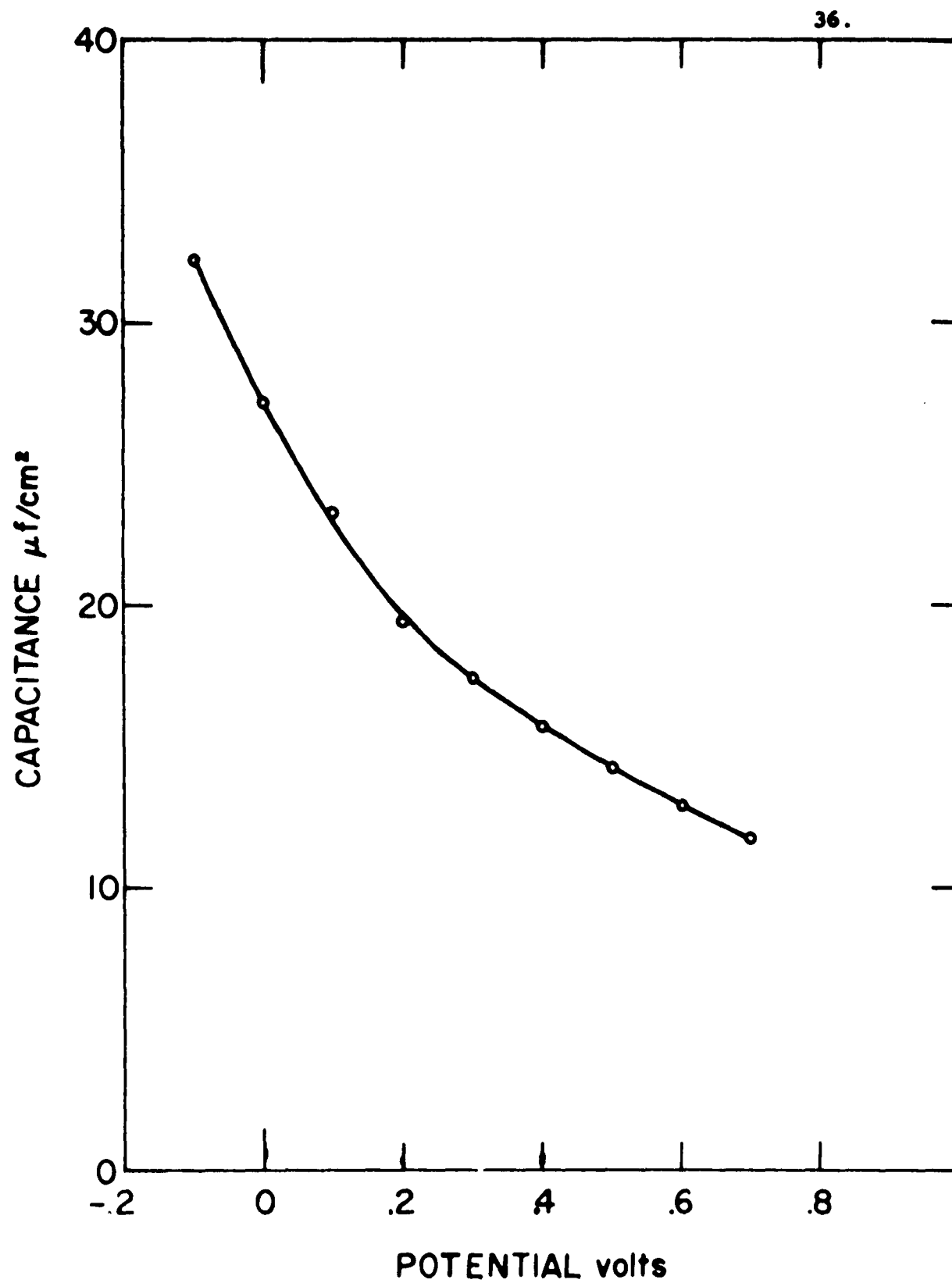


Fig. 12. Capacitance versus potential.

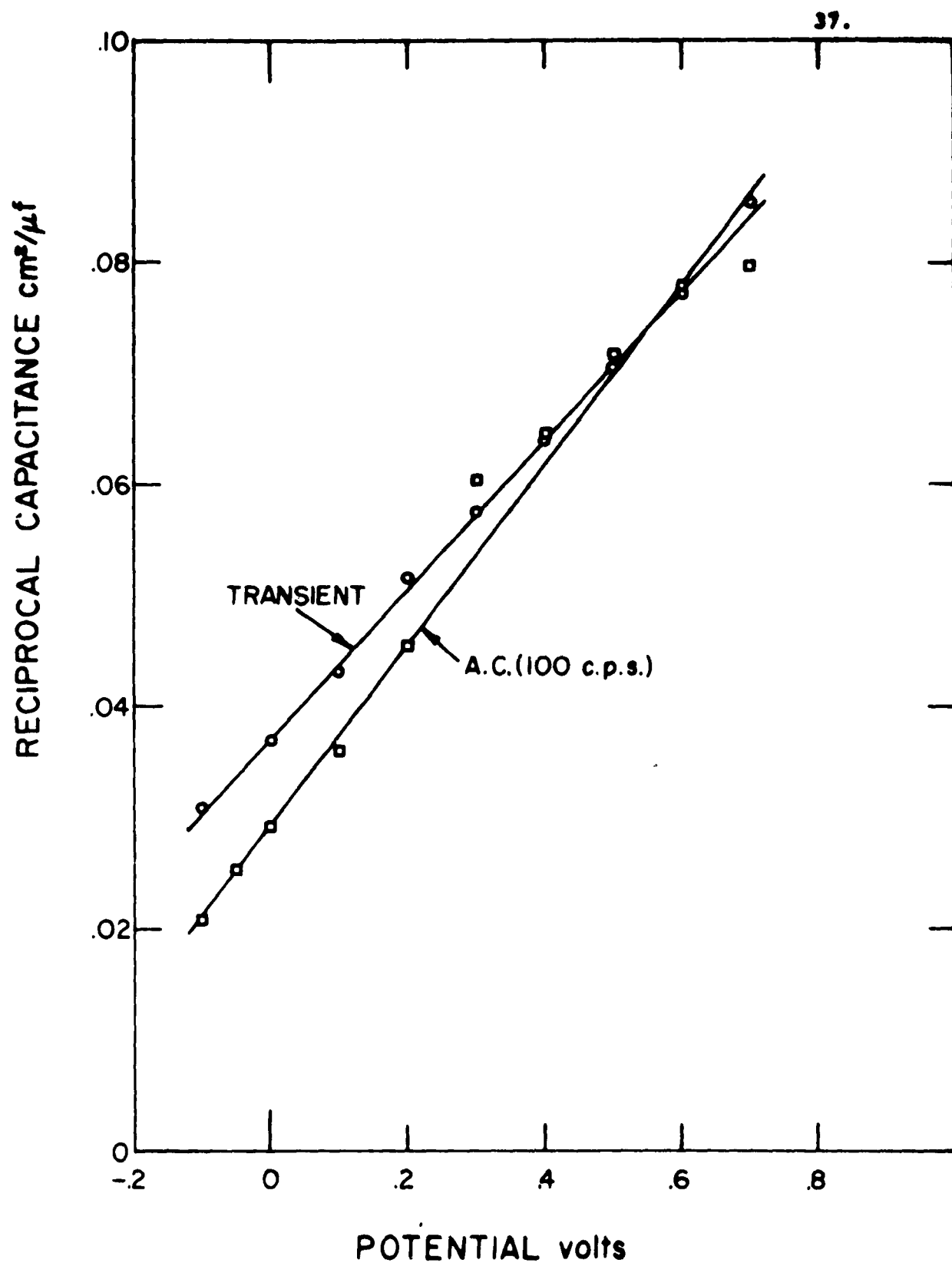


Fig. 13. Reciprocal capacitance versus potential.

zero of overpotential.  $v_o^*$  depends only on overpotential for concentrations of  $H_2SO_4$  between .01 N and 10 N. The concentration dependence of the steady-state current plotted in Fig. 5 is reflected only in the concentration dependence of the  $i_o$  factor.

The temperature dependence of the overpotential parameters also emphasizes the importance of  $i_o$ . Open-circuit transients taken in conjunction with the measurement of the temperature dependence of the steady-state current show that  $v_o$  changes by less than 10% over the temperature range from 0° C to 40° C, which is consistent with a proportionality to  $kT$ .

## V. THE PASSIVE STATE TO ACTIVE STATE TRANSITION

The transition from the passive state to the active state under open-circuit conditions was displayed in Fig. 8. Somewhat similar curves are obtained for all galvanostatic transients in which the current is less than the steady-state current. Included in this category are anodic currents less than the steady-state current (anodic reduction), and all cathodic currents (cathodic reduction). The term "reduction" is not intended to imply that the reaction involved is reduction of an anodic layer, although this may be the case to some extent. Two types of measurement can be used to study the transition. Curves can be obtained for various reduction currents, and their shape can be studied as a function of the reduction current. Alternately, the transition can be interrupted, and the repair transient can be recorded.

Two cathodic reduction transients are presented in Fig. 14. The charge co-ordinate is defined as the difference between the steady-state current and the reduction current multiplied by time. Potential is plotted versus charge rather than time so that both curves can be plotted in the same figure. The general features of the shape of reduction transients can be described using two parameters: the shift in the plateau potential, and the charge required to activate the electrode.

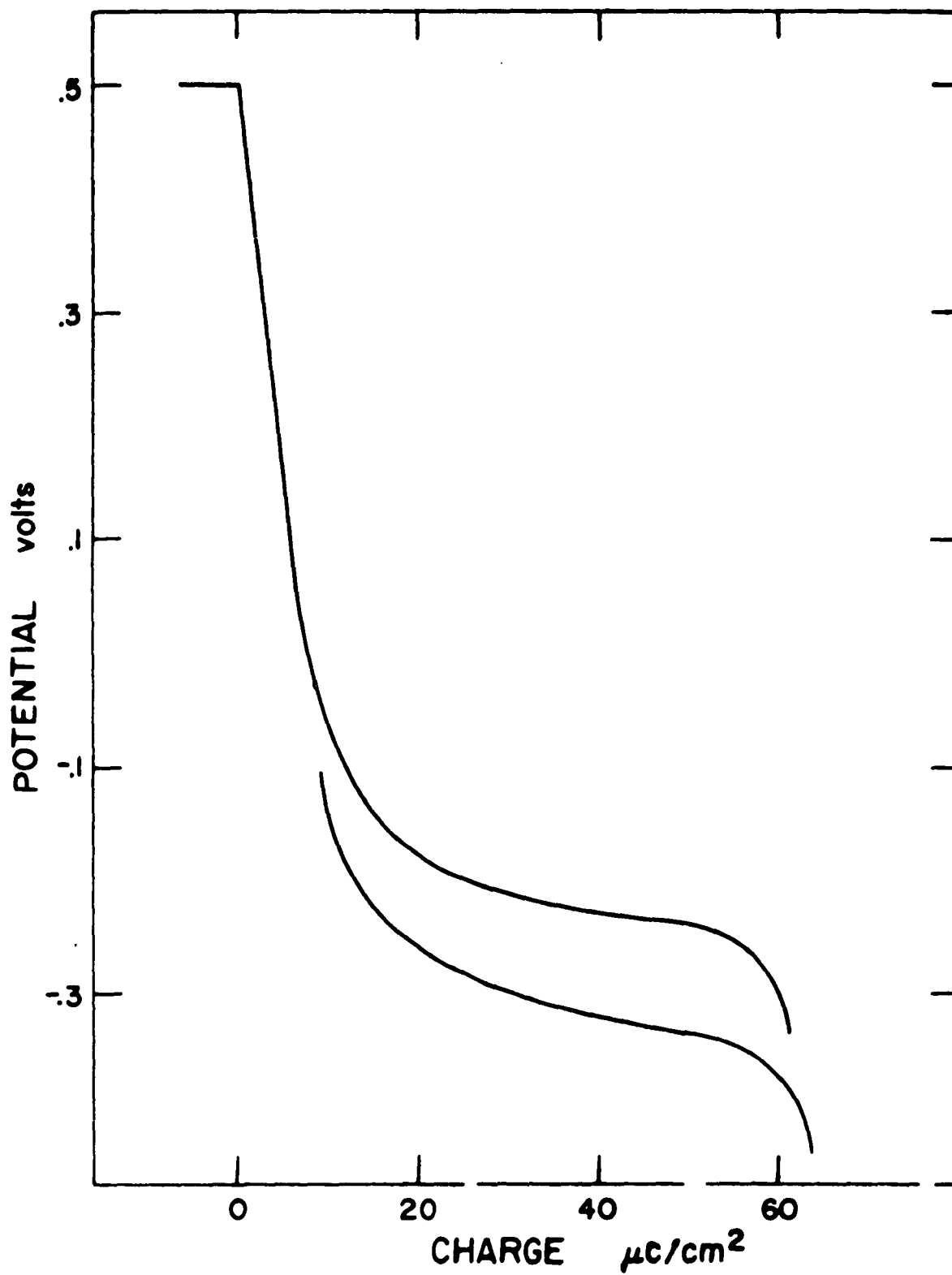


Fig. 14. Cathodic-reduction potential transients. Reduction current: upper curve,  $.256 \text{ ma}/\text{cm}^2$ ; lower curve,  $2.56 \text{ ma}/\text{cm}^2$ .

The potential plateau shifts to more negative potentials as the cathodic reduction current is increased in magnitude. If the circuit is opened during a cathodic reduction transient, the potential rises along a capacitive transient from a point on the reduction plateau to a point on the open-circuit plateau. The plateau shift is, therefore, an overpotential associated with the electrode activation reaction. A plot of the plateau shift versus reduction current shows a logarithmic dependence. Hence current and potential are related by an equation similar to Eq. (5). The  $v_o$  parameter of this relation can be determined directly from the plateau shift and the ratio of the reduction currents if the  $i_o$  parameter is assumed independent of current.  $v_o$  rises from .038 volts at a passivating potential of .1 volts to .048 volts at a passivating potential of .5 volts. There is no similarity between the behavior of this parameter and the behavior of the  $v_o$  parameter associated with the forward current and plotted in Fig. 11.

Fig. 14 shows two cathodic reduction transients with greatly different reduction currents. The charge required to activate the electrode is approximately the same for both. Fig. 15 shows the dependence of the charge required to activate the electrode upon reduction current. No attempt is made to distinguish between points taken at different potentials. For sufficiently large currents the charge is independent of both passivating potential and reduction



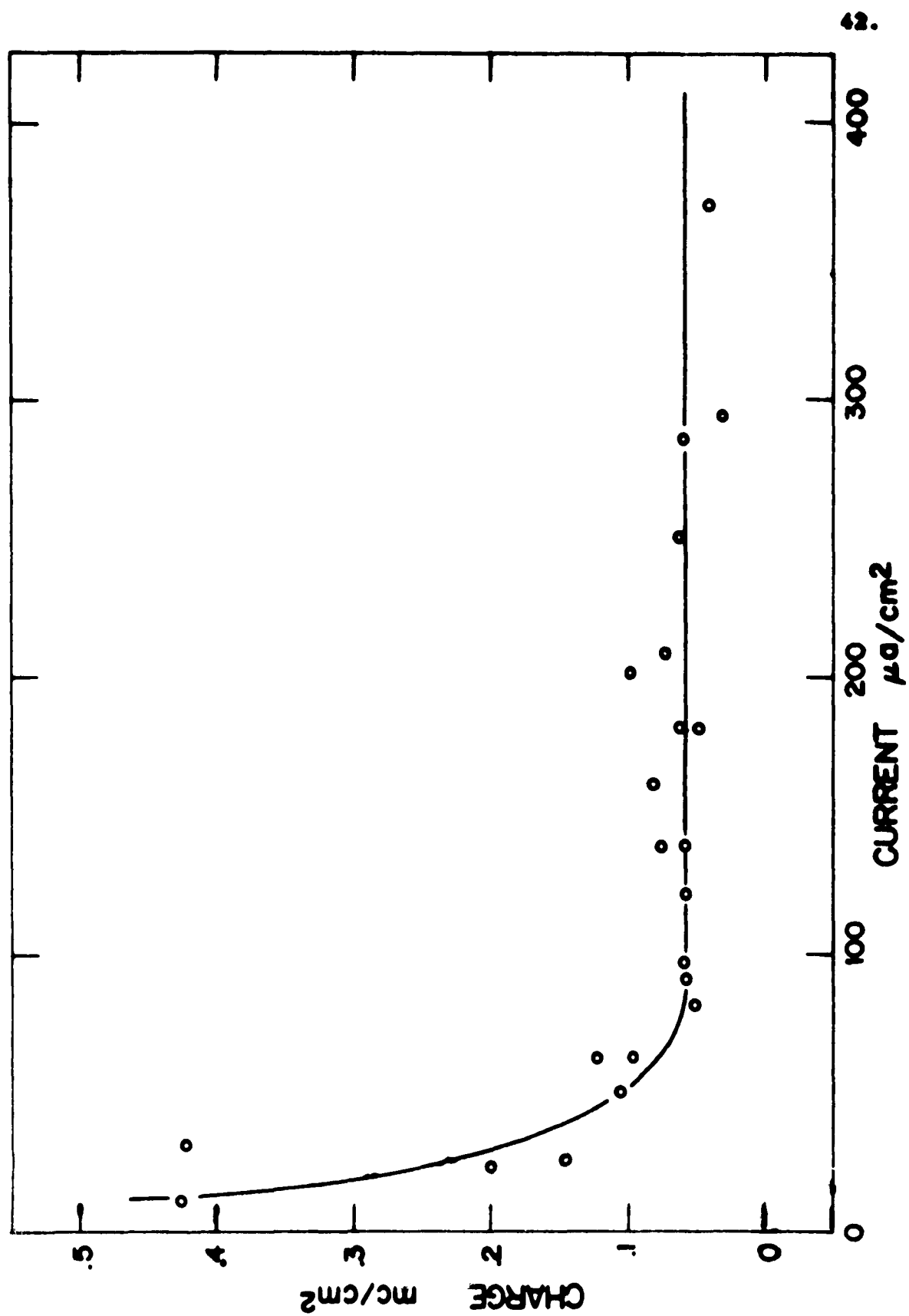


Fig. 15. Charge to activate versus cathodic reduction current.

current. The two curves shown in Fig. 14 indicate that the charge remains independent of current for currents larger than those plotted in Fig. 15. At smaller values of the current the charge begins to rise. The charge rises steeply as the current passes into the anodic region, and starts to show a potential dependence. Fig. 16 shows that at constant anodic reduction current the charge depends linearly on the passivating potential. This result indicates that the transition to the active state involves change in thickness of the passive layer for reduction currents in the anodic region. The anodic region has not been studied in detail due to the tendency for the cell to become unstable. The steepness in the slope of the charge versus current curve at zero current accounts for the rather large amount of scatter observed in the time required to reach the active state under open-circuit conditions.

Transients applied along the plateau provide some additional information on the electrode activation reaction. Fig. 17 shows the current transient observed when the circuit is closed after being open for 40 seconds. (Only the part after the large initial spike is shown.) This is a potentiostatic transient involving a large discontinuity in potential. A comparable potentiostatic transient starting from a steady state is shown in Fig. 20 in the next section. The transients are comparable in that they both involve switching to the same constant potential, but the transient

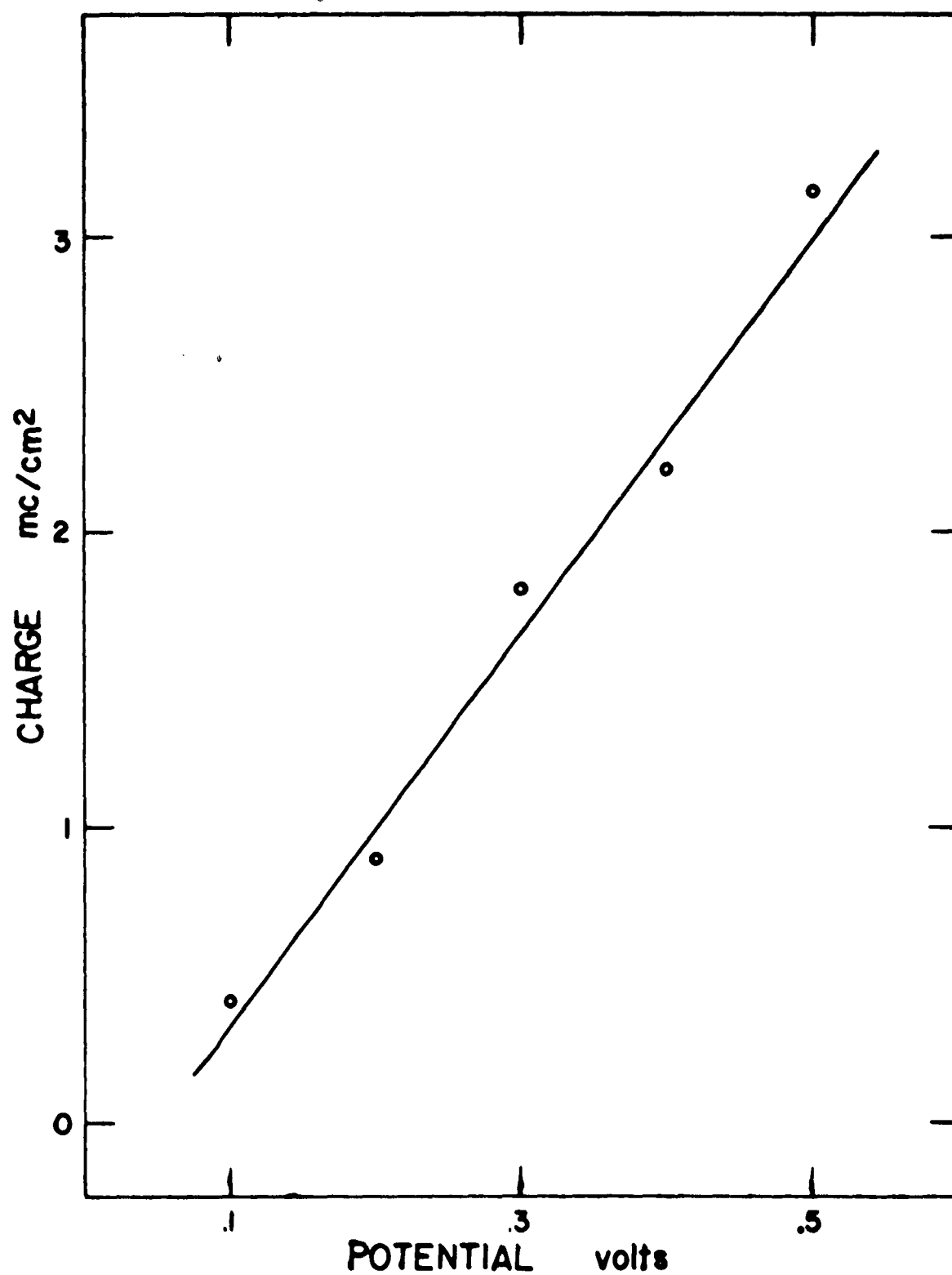


Fig. 16. Charge to activate versus potential. Anodic reduction current,  $3 \mu\text{a}/\text{cm}^2$ .

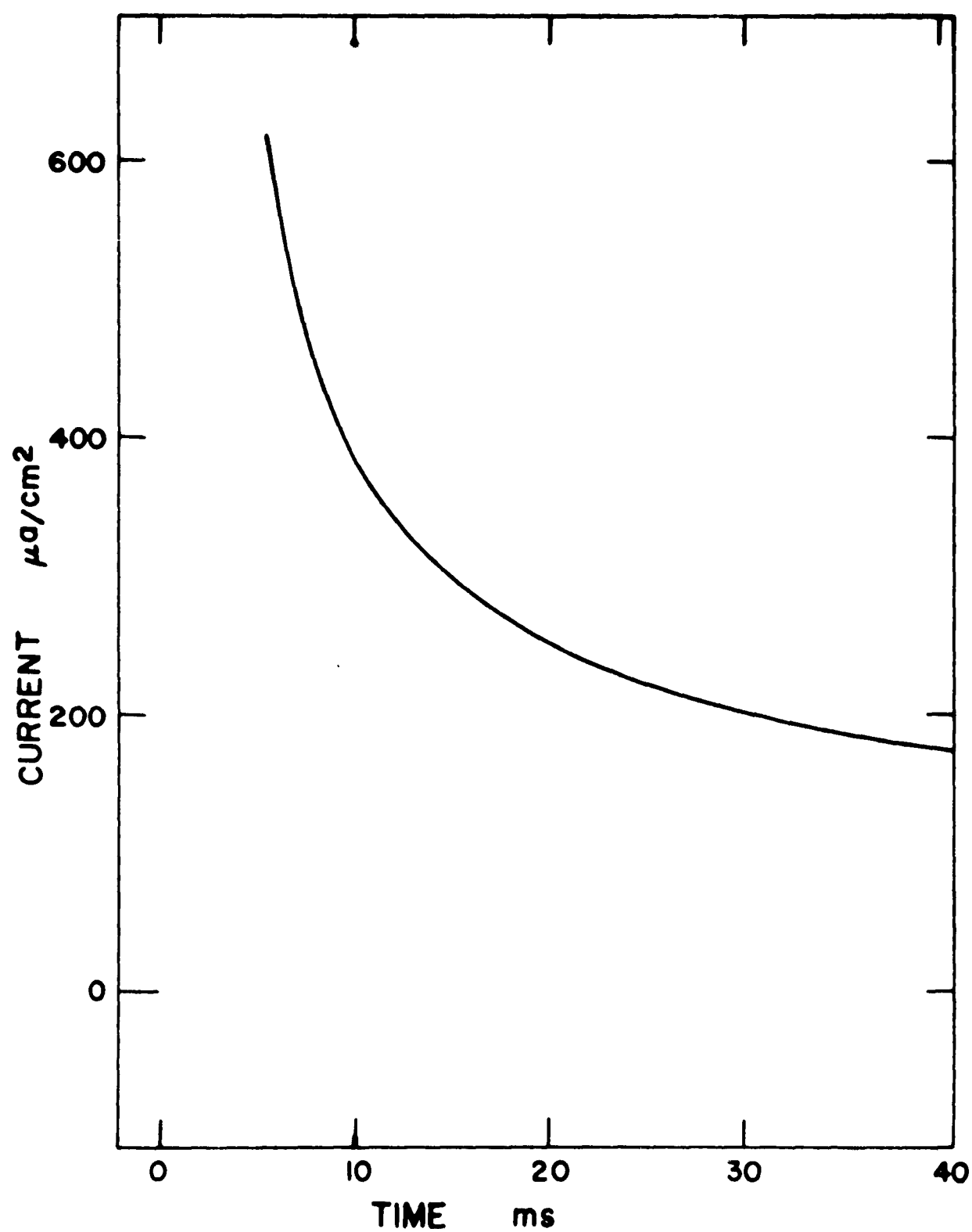
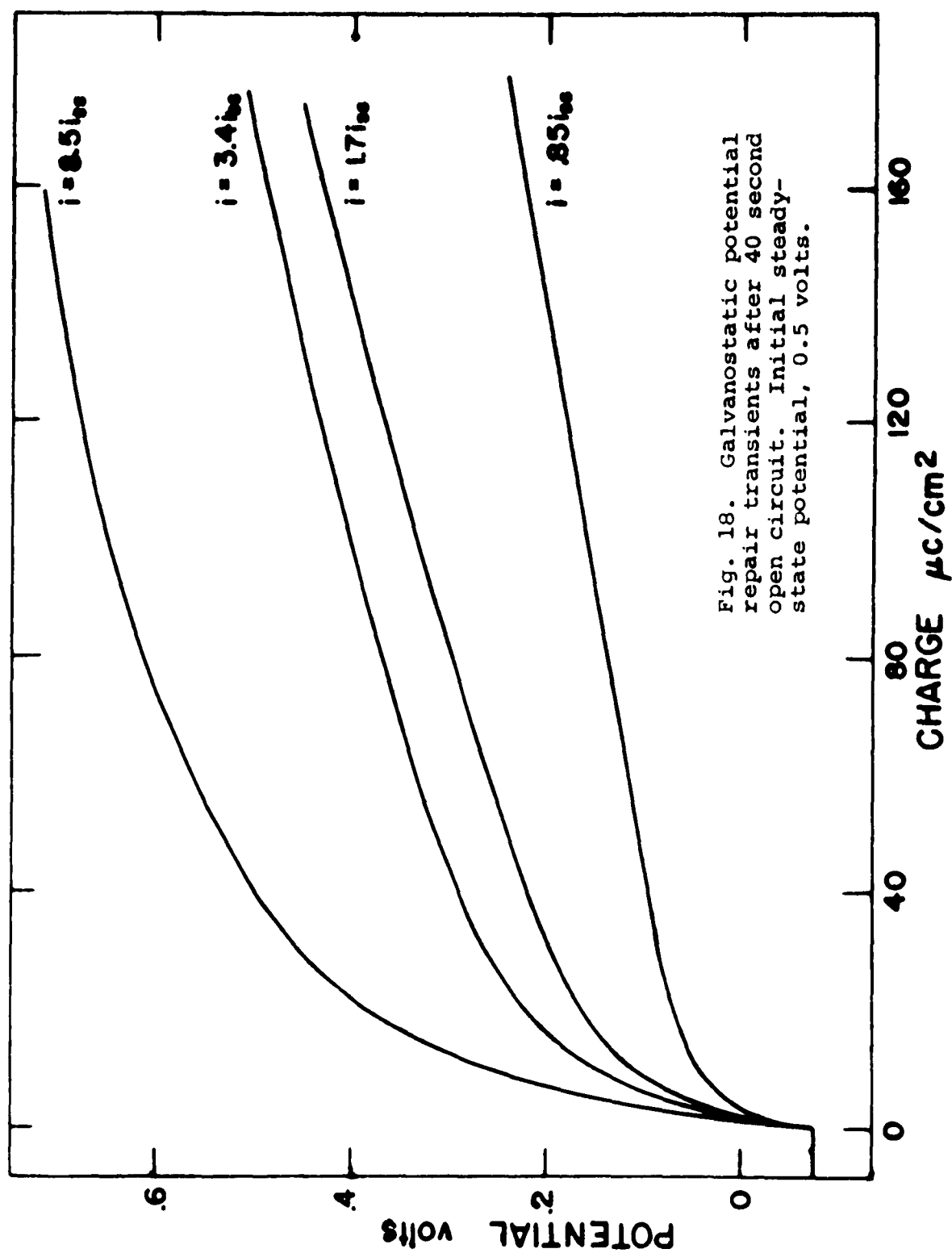


Fig. 17. Potentiostatic current repair transient after 40 second open circuit. Potential, .5 volts.

which starts from a steady state (of necessity) involves a smaller discontinuity in potential. The time constant of the repair transient from the plateau is more than two orders of magnitude faster than that of the transient starting from the steady state. (The wide disparity between the time constants is observed even for a repair transient which is applied at the end of the plateau just before the sharp transition to the active state.) More general potentiostatic transients can also be applied along the plateau. For potentials less than or equal to the initial passivating potential, transients similar to Fig. 17 are obtained. For higher potentials the transients are nearer to Fig. 20 in appearance. These results indicate that for zero or negative reduction current the electrode retains some feature characteristic of its initial passivating potential as it undergoes the transition to the active state. This conclusion is consistent with the assumption that for these reduction currents the thickness of the passive layer does not change as the electrode is activated

The repair process can be studied more easily using galvanostatic transients, since here the events occur slowly. Fig. 18 shows such transients taken after the circuit has been open for 40 seconds. The charge plotted as abscissa is defined as the current-time product. This definition differs from the definition used for Fig. 15. The change in definition is necessitated by the observation

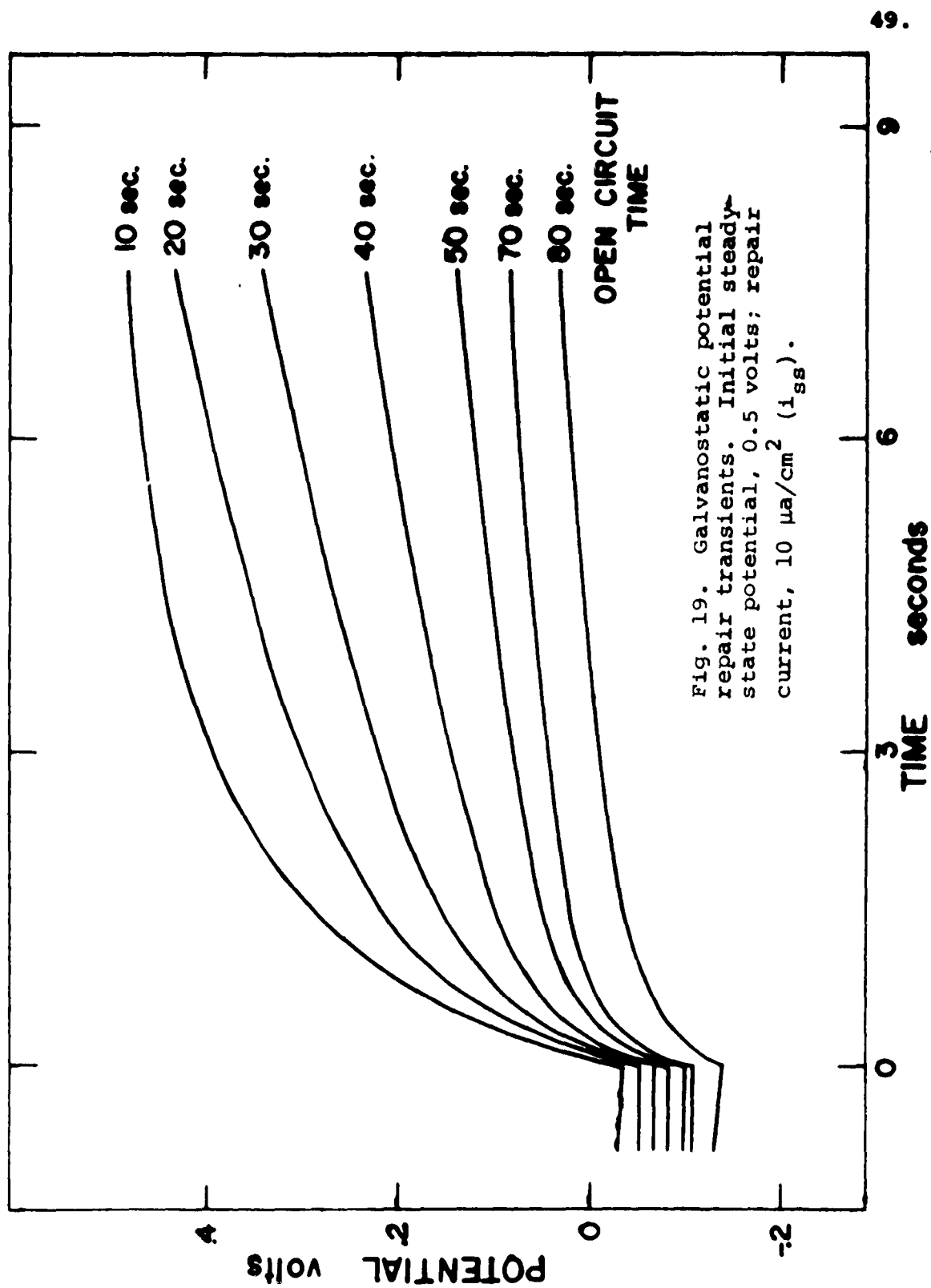


that the rapid transition to the active state which takes place without thickness change for cathodic reduction currents can be arrested by applying an anodic current less than the steady-state current. When such an anodic current is applied at a point on the open-circuit plateau, first the damage to the layer caused by the rapid activation reaction is repaired, and then the electrode goes through the slow transition to the active state characteristic of anodic reduction.

Fig. 19 shows repair transients taken at various open-circuit times with the repair current equal to the steady-state current. The curvature of the plateau indicates that on the lowest curve the electrode would have activated within a second or two had not the steady-state current been re-applied.

A quantitative determination of the behavior of the overpotential parameters as the electrode is activated is not attempted here because of the complications which arise when currents greater than the steady-state current are applied. These complications are described in the next section.

The work on the passive to active transition described in this section agrees with work done earlier by Weil.<sup>12/</sup> There appear to be two different mechanisms by which the electrode can reach the active state. Under anodic reduction the layer becomes uniformly thinner until the active state is reached. Under cathodic reduction the electrode reaches





the active state rapidly without change in thickness of the passive layer. Weil assumes that the rapid activation process corresponds to creation of a hole in the layer, but this process should have some thickness dependence, and none is observed.

## VI. KINETICS OF FORMATION AND REMOVAL OF THE PASSIVE LAYER

The determination of the kinetics of formation and removal of the passive layer is in general a complicated problem. We have obtained evidence to support the assumption that a layer of variable thickness is present at the electrode-electrolyte interface. The dependence of thickness upon passivating potential is assumed to be given, except for the proportionality constant, by the plot of  $v_o$  versus potential shown in Fig. 11. In the preceding section we studied the transition from the passive state to the active state and found that appreciable thinning occurred only under anodic reduction. In the present section further studies are made of the kinetics, and are concerned mainly with the formation and thickening of the passive layer.

A simple theory of thickness change can be derived starting from the assumption that the rate of change of thickness of the layer is proportional to the excess in current over its steady-state value. This assumption is expressed in the equation

$$dD/dt = K(i - i_{ss}) \quad , \quad (9)$$

where  $D$  is the thickness of the layer, and  $K$  is a constant. Either potentiostatic or galvanostatic transients can be used to study thickness change. The unavoidable current spike makes potentiostatic transients unsuitable for a quantitative study of thickness change, but they do provide qualitative information about the process.

Starting from the steady state, let us consider two potentiostatic transients, one where the potential has been raised to a higher value, and the other where the potential has been decreased to a lower value. Because of the exponential dependence of current upon potential (Eq. (5)), the average current flowing during the first transient will be much greater than that flowing during the second transient. Therefore, according to Eq. (9) the thickening in the first case will take place much faster than the thinning in the second case. This behavior is observed experimentally; when the potential is switched up the time constant of the transient is on the order of ten minutes, whereas on lowering the potential the time constant is on the order of one hour. Franck and Weil<sup>5/</sup> passivate using constant current and reach the oxygen-evolution region before switching the potential down to a value in the passive region. This technique requires that the layer become a great deal thinner before a steady state is reached, and hence they find that a long time is required before the electrode reaches a steady state.

A typical potentiostatic transient is presented in Fig. 20. The initial potential is .12 volts and the potential increment is .38 volts. This figure can be compared to Fig. 17, the potentiostatic repair transient from the open-circuit plateau. The vertical scales are identical, but the time axes differ by a factor of 200.

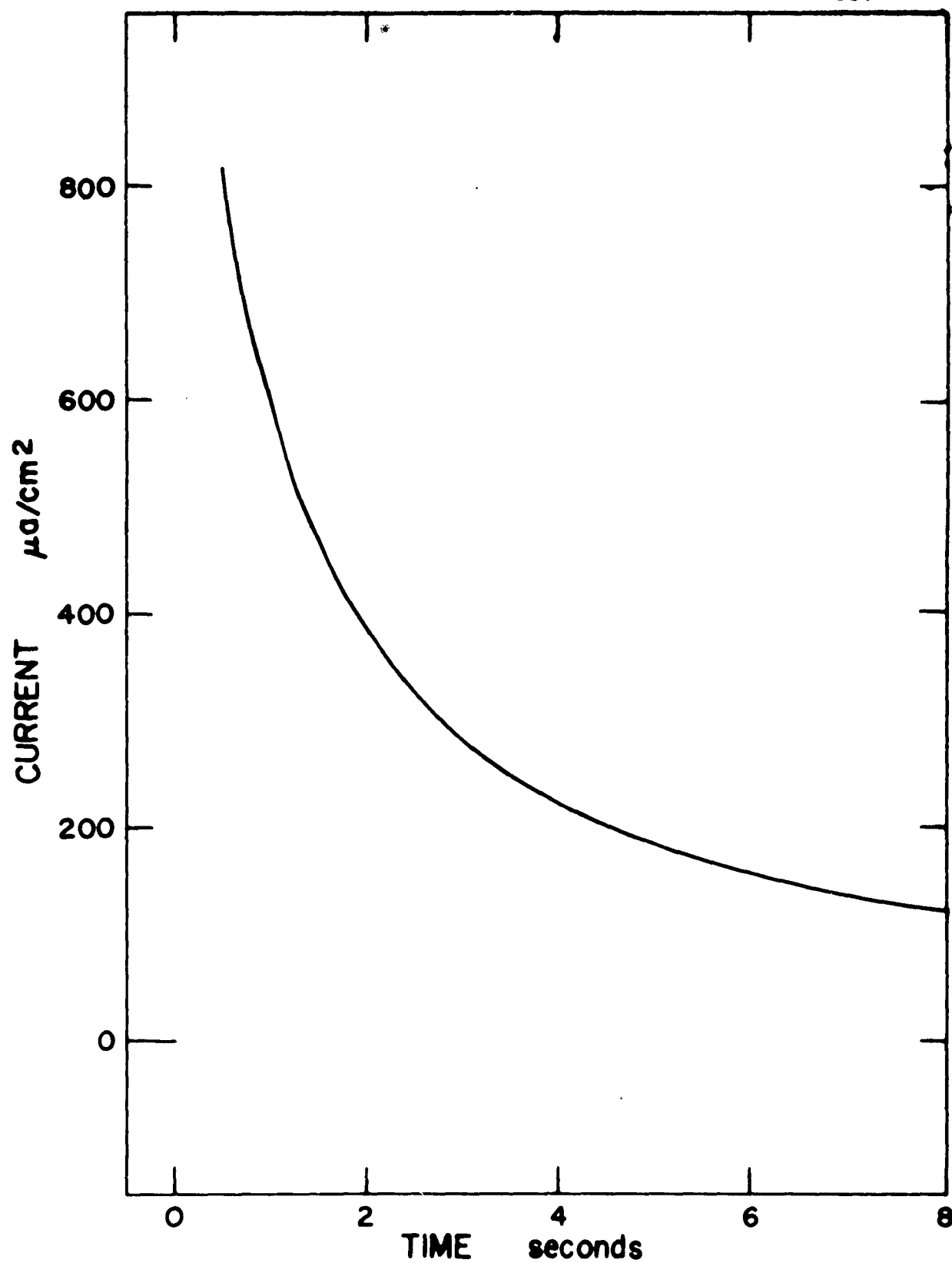


Fig. 20. Potentiostatic current transient. Initial steady-state potential, .12 volts, potential increment, .30 volts.

Except for the difference in time constant the curves are roughly similar in shape. This difference in time constant shows that the repair process can involve little change in thickness. The potentiostatic thickening transient is complicated at higher initial steady-state potentials by the appearance of an undershoot after the capacitive transient. This undershoot corresponds roughly to the potential overshoot in the galvanostatic transients described below.

Galvanostatic transients must be used for a quantitative study of thickness change, and a typical one is shown in Fig. 21. The initial capacitive transient is followed by a plateau, and then the potential begins to rise linearly with time. There is a tendency to overshoot, which is greatest for initial potentials in the middle of the passive region, and goes to zero near both ends of the passive region. For potentials at which overshoot occurs, it is observed for all values of the current. Fig. 22 shows, on an expanded scale, a transient exhibiting overshoot.

At high passivating potentials the length of the plateau shows little potential dependence. It varies approximately inversely with excess current, indicating that a constant amount of charge is required to reach the end of the plateau. At lower potentials the length of the plateau tends to zero. At still lower potentials the transient becomes more complicated as the steady-state current becomes dependent upon potential

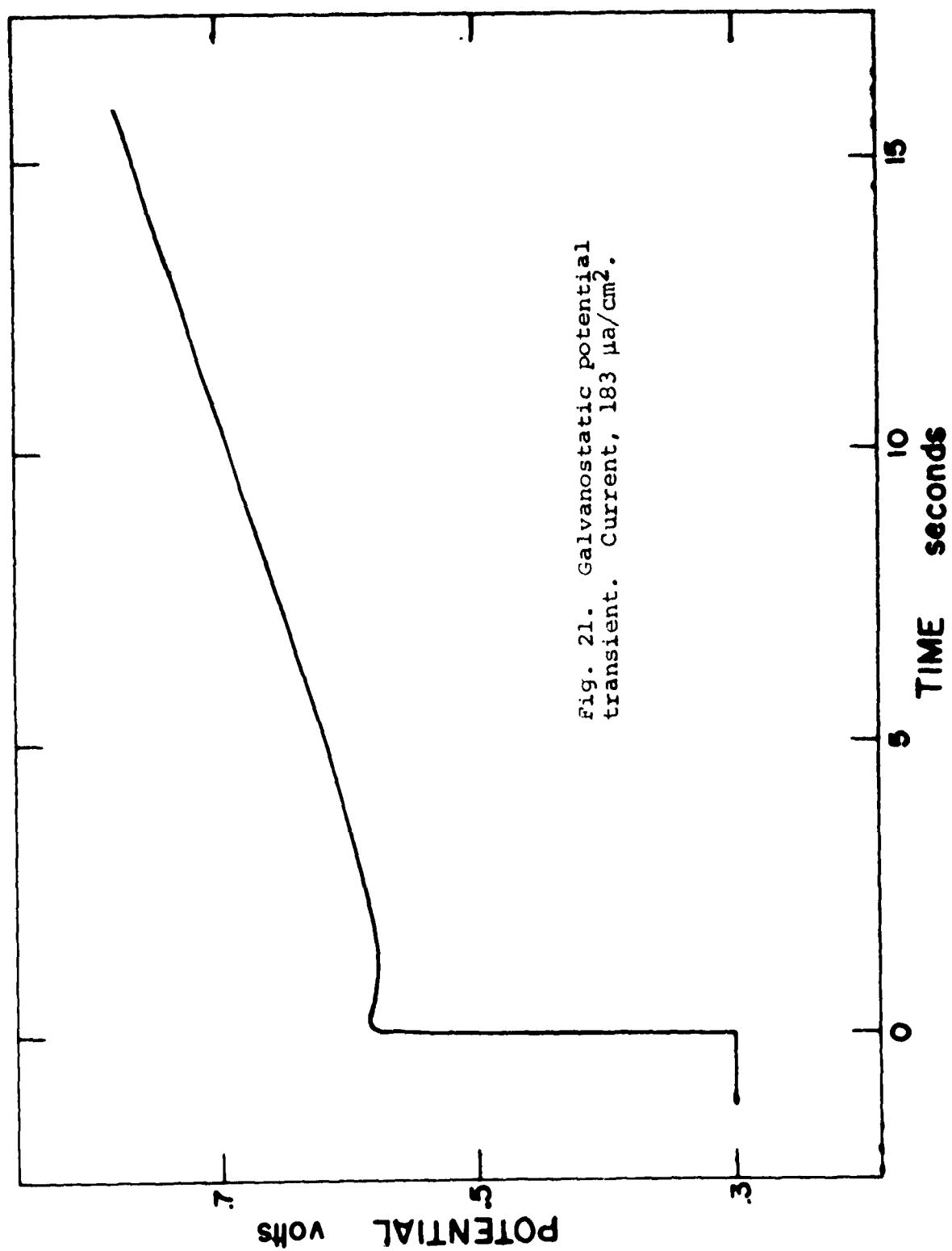
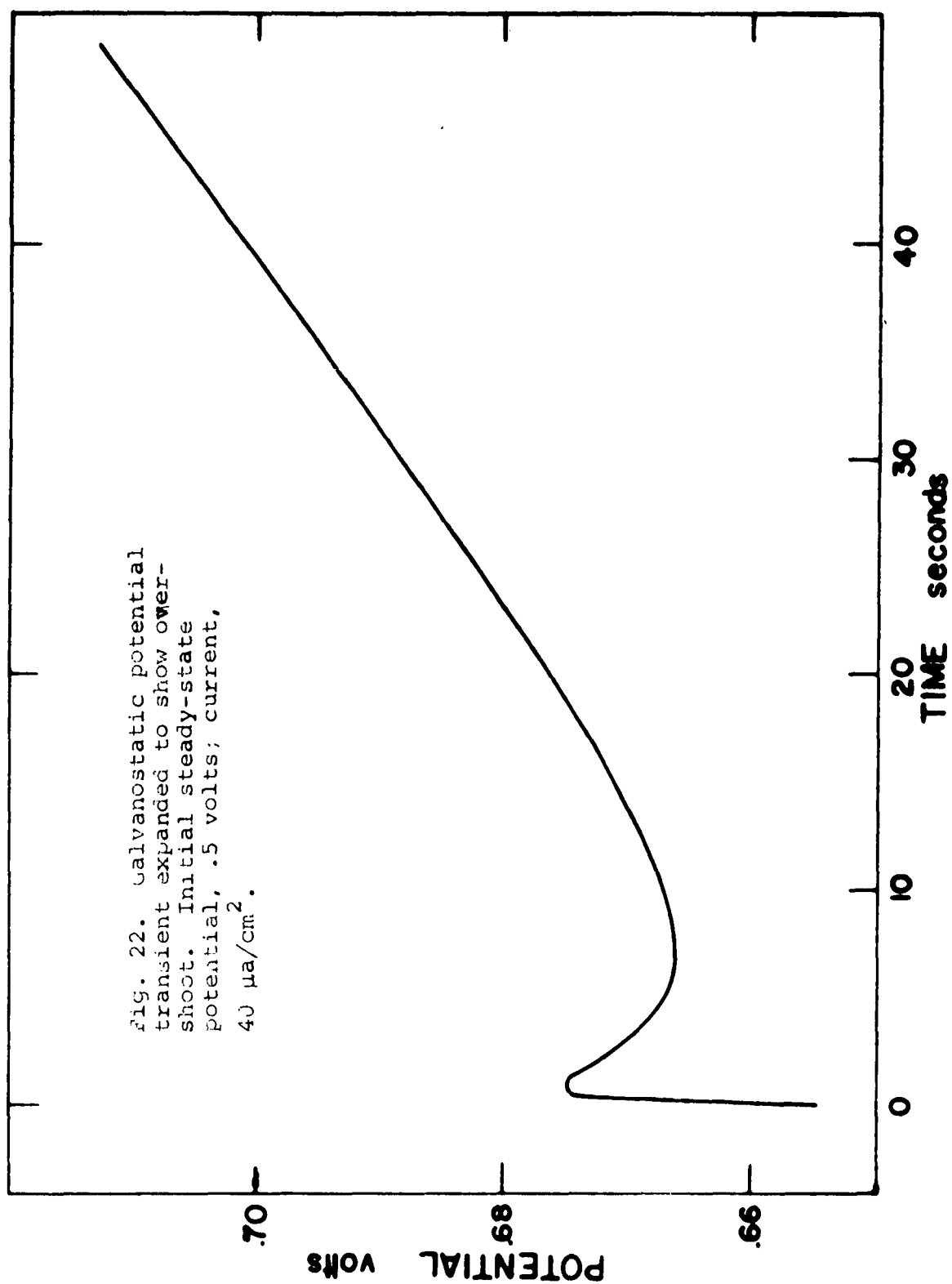


Fig. 21. Galvanostatic potential transient. Current,  $183 \mu\text{A}/\text{cm}^2$ .



The slope of the linear rise in Fig. 21 would appear to be a good experimental parameter to use for a quantitative study of thickness change. A logical approach would be to identify  $v_0$  with  $D$  in Eq. (9), and to solve Eq. (6) and Eq. (9) for the slope of the rise. This calculation can be carried out, but the current dependence of the slope does not agree with the experimentally observed one. The overshoot and the plateau suggest that something is happening in addition to thickness change.

In section 4 the overpotential parameters were found to be good parameters, i.e., independent of current and potential, over all of the open-circuit capacitive transient except for the first few millivolts. The experiments, used to study thickness change, employ currents which are much greater than the steady-state current, and hence it is necessary to study the parameters to see whether an extrapolation from the low current behavior is valid, before attempting a quantitative study of thickness change.

The method most commonly used to determine the  $v_0$  parameter in an exponential relation such as Eq. (5) is the "rapid" method.<sup>10/</sup> Ordinary activation-controlled electrochemical reactions are usually studied by recording the potential for a number of values of the current. For currents which are several times the exchange current, the  $v_0$  parameter can be determined from

$$v'_0 = (v_2 - v_1) / \ln(i_2/i_1). \quad (10)$$



The only assumption involved in this equation is that the parameters are true parameters and do not depend on current. Since this assumption does not turn out to be valid in this application, the parameter is designated  $v'_0$ , not  $v_0$ . When this method is applied to the case where a layer is present, the measurement must be performed rapidly so that the thickness of the layer does not change, and hence the name "rapid" method. The results of applying this method to the passive iron electrode are plotted in Fig. 23. The  $v'_0$  parameter is fairly well defined, that is, it is approximately independent of the current used to obtain it. Fig. 23 is not similar to Fig. 11, the corresponding plot of  $v_0$ ; in fact the two curves cross near a passivating potential of .2 volts. From this information it can be concluded that one or both of the overpotential parameters must depend on current.

Further information is obtained by opening the circuit after the current is raised. A constant current is applied until an excess charge of .05 mc has reached the electrode, and then the circuit is opened and the shape of the capacitive transient analyzed. (The excess charge is held constant as the current is varied so that the effect of any thickness change will cancel out. Later in this section it is shown that .05 mc causes negligible thickness change anyway, yet it is sufficient charge to complete the capacitive transient.) The open-circuit transient is also

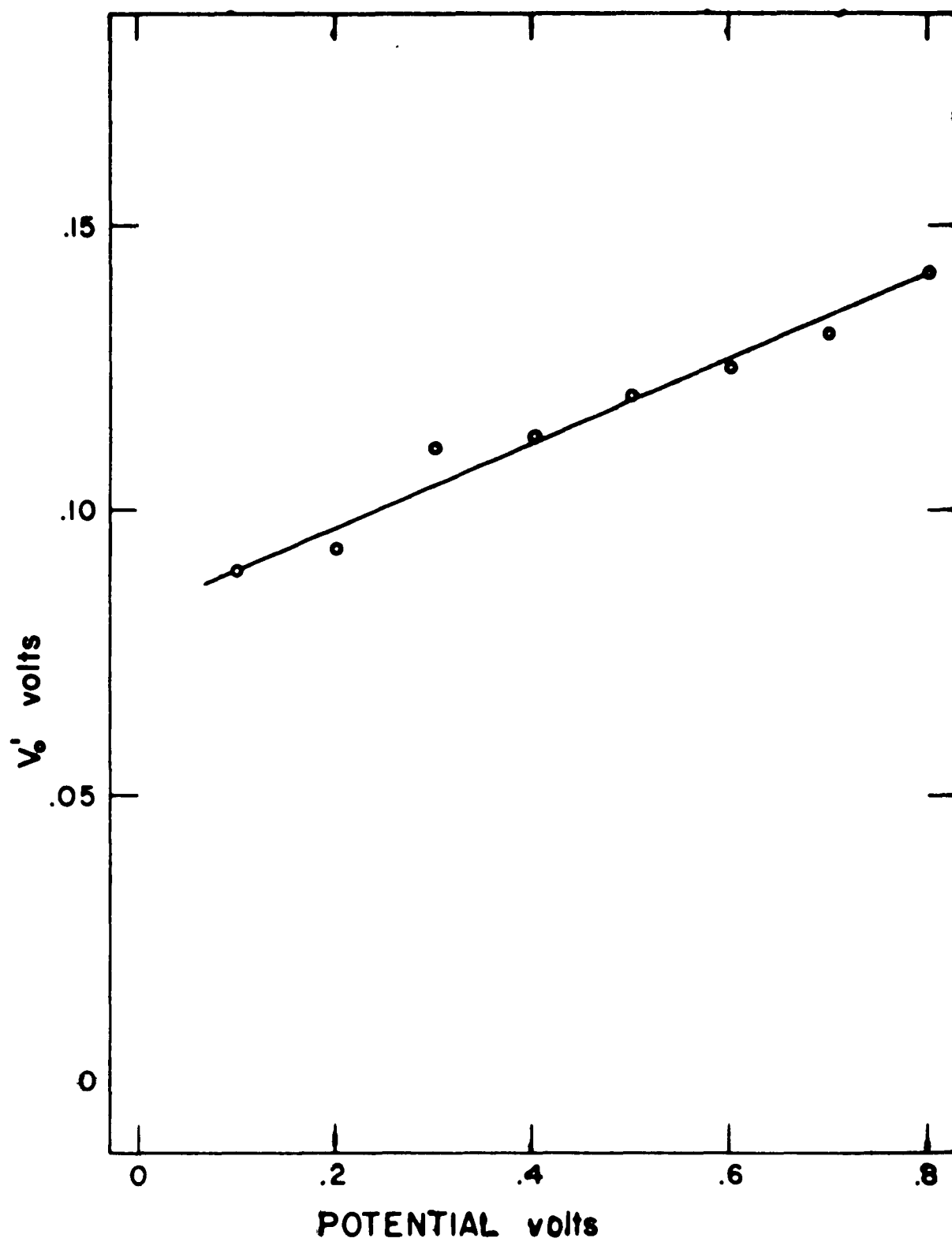


Fig. 25.  $V_0'$  versus potential. Current,  $22 \mu\text{a}/\text{cm}^2$ .

found to fit a  $\ln(t + \theta)$  function. The region over which it does includes currents lower than the steady-state current. The results of this experiment are plotted in Fig. 24 and Fig. 25. The way in which the overpotential parameters vary with current depends upon whether the initial passivating potential  $v_i$  is above or below the crossover point of Fig. 11 and Fig. 23. For  $v_i = 0.1$  volts,  $v_o$  and  $i_o$  both rise with increasing current; for  $v_i = 0.5$  volts,  $v_o$  and  $i_o$  both fall with increasing current.

At first sight, these results seem strange. According to Fig. 23, the overpotential parameters must change rapidly when the current is raised above its steady-state value. But when the circuit is opened, these parameters stay approximately constant as the potential decays to well below its steady-state value.

To understand this, let us make a slightly different experiment. Instead of opening the circuit, let us switch the current back to its steady-state value. The resulting transient is shown in Fig. 26. At first, there is a fast capacitive transient, followed by a slow undershoot. Since enough charge was added originally, the layer has thickened appreciably and the potential rises in about half a minute to a final value consistent with this thickness.

In view of the fact that the time to this final state is long in comparison to the time constant of an open-circuit transient, it might be expected that the  $v_o$  parameter would

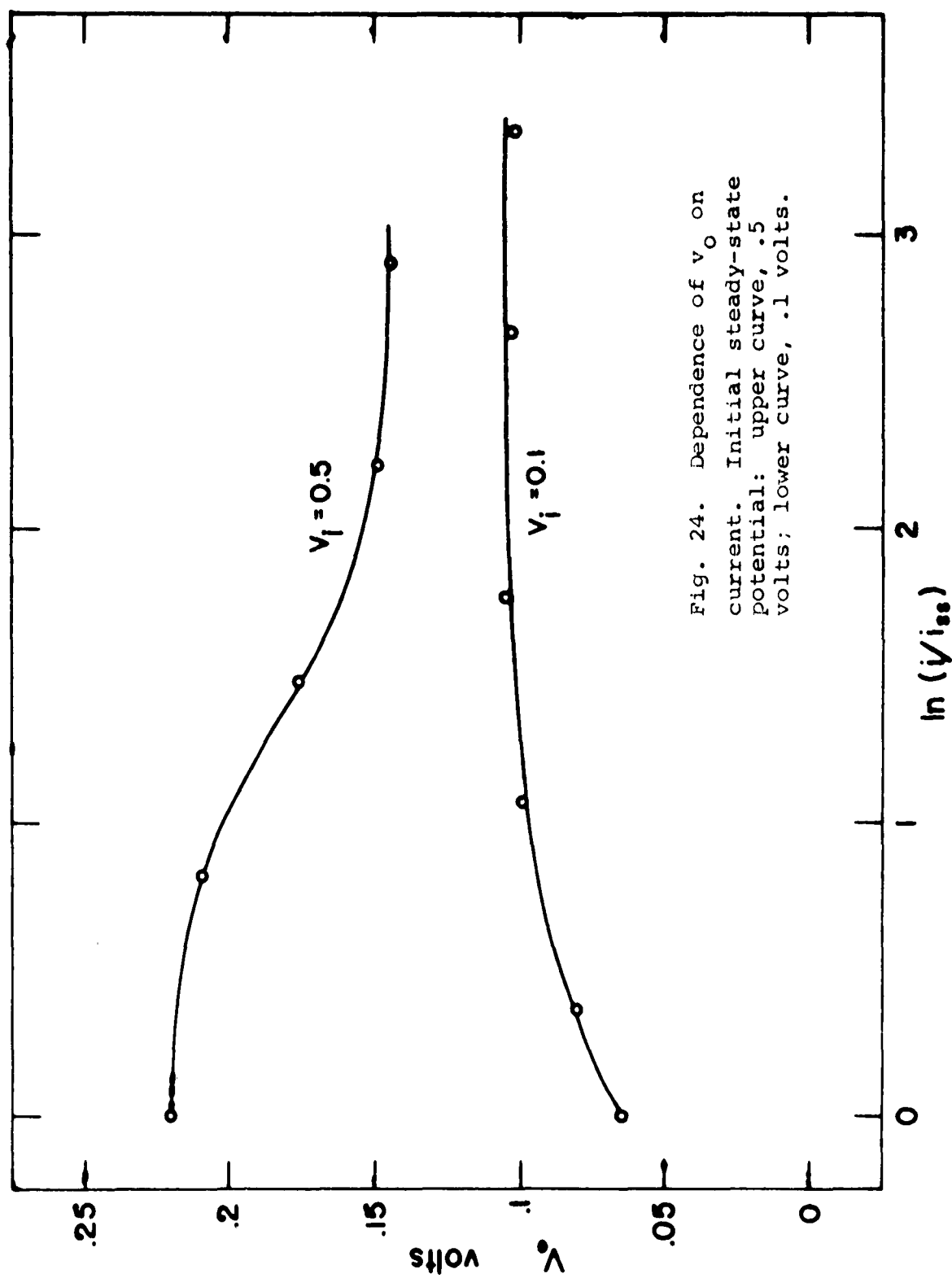
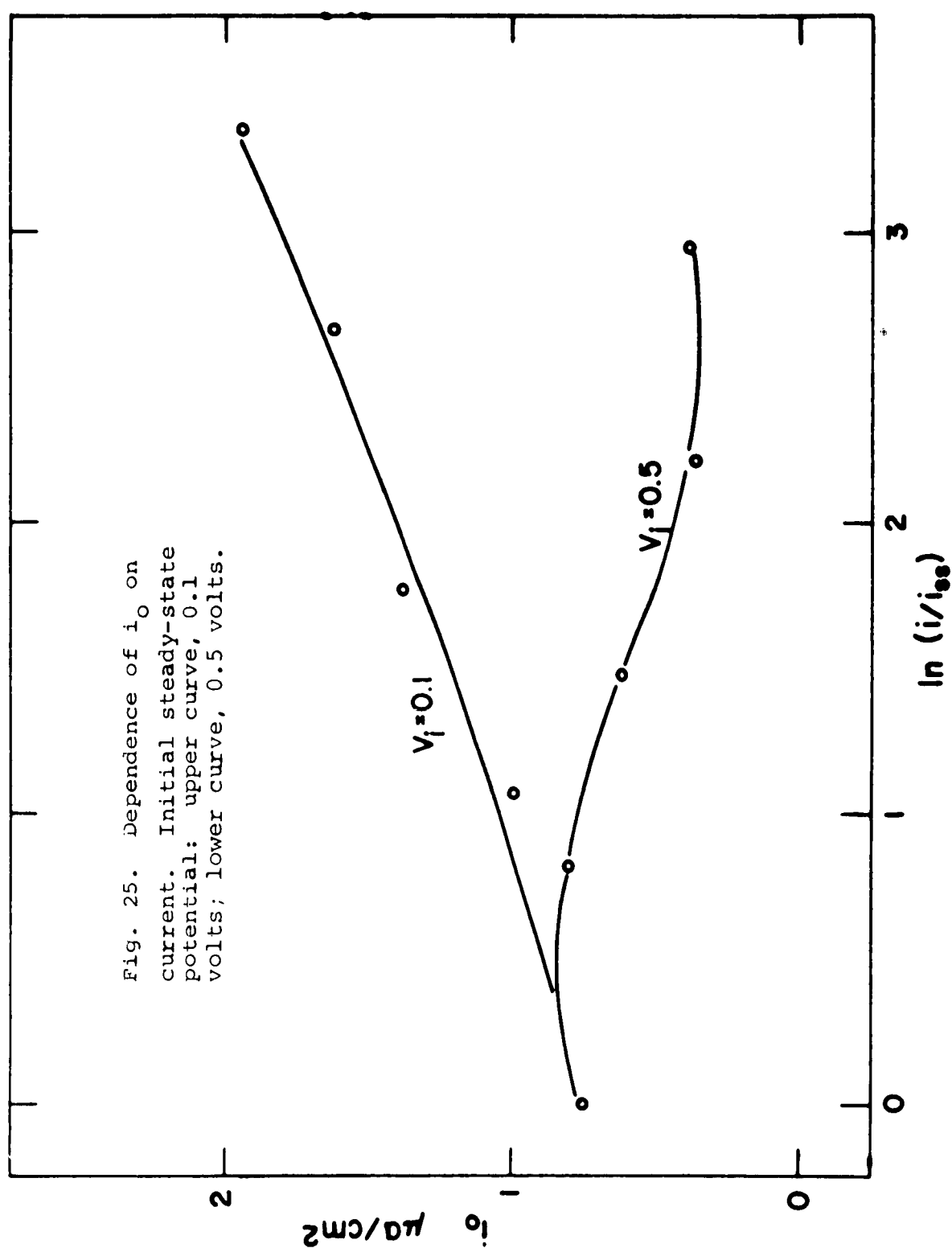
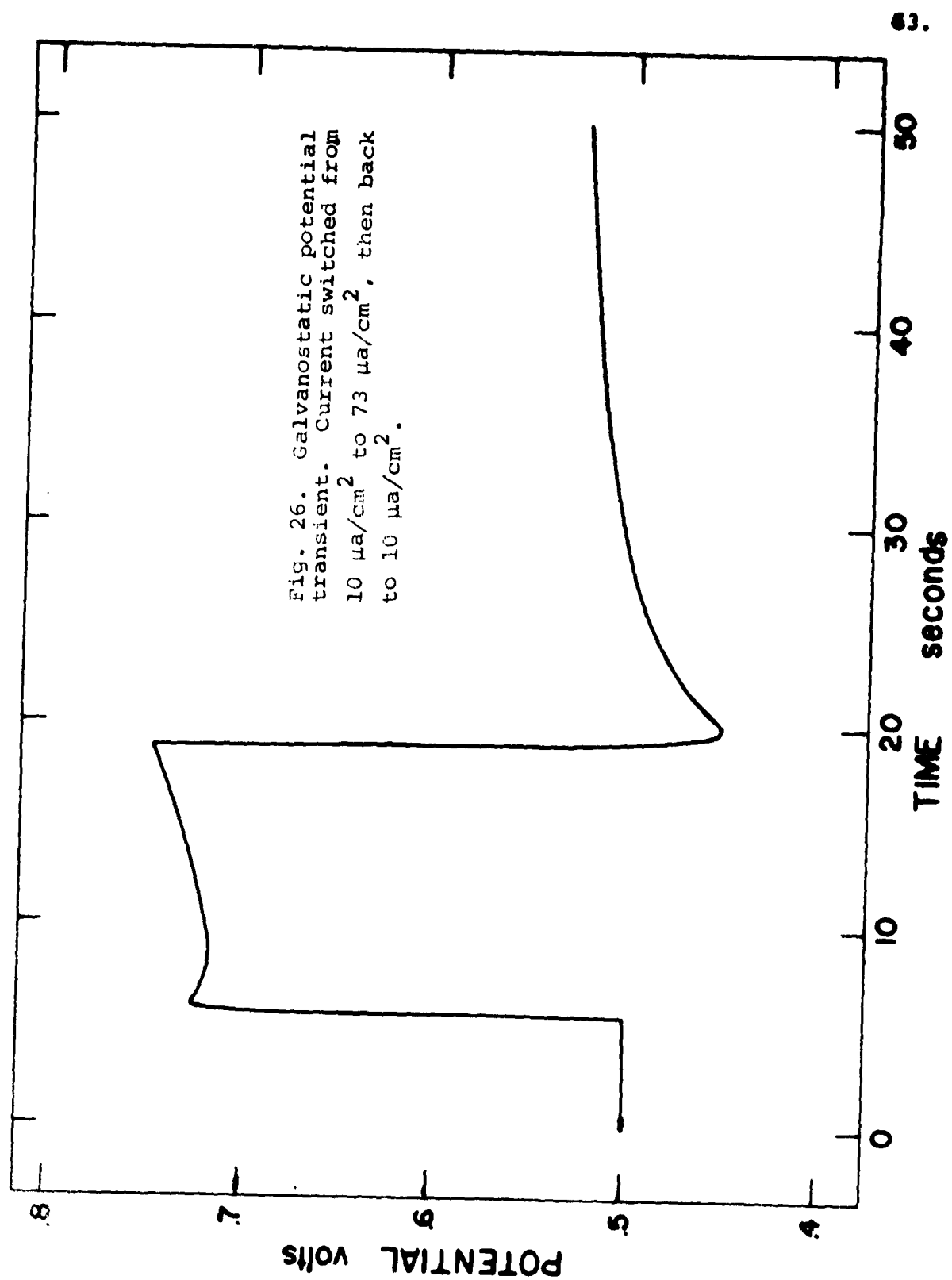


Fig. 24. Dependence of  $v_o$  on current. Initial steady-state potential: upper curve, .5 volts; lower curve, .1 volts.





show little change over the course of the open-circuit transient, and this is what is observed.

The study of thickness change is greatly complicated by the current dependence of the overpotential parameters. In spite of the additional complexity of the equations describing the thickening process, the assumption involved in Eq. (9) can be tested by a very simple experiment. Transients similar to Fig. 26 can be recorded for fixed charge increments, and the potential at which the system becomes stable can be plotted as a function of charge. (A brief open-circuit transient can be recorded after the system becomes stable and  $v_0$  can be obtained, but this complicates the transient and only serves to reproduce Fig. 11.) The results of this experiment are plotted in Fig. 27. The potential rises linearly with the excess charge reaching the electrode at a slope of  $.0415 \text{ volt-cm}^2/\text{mc}$ . This result supports the concept of a variable thickness layer. It makes possible a calculation of the thickness of the layer provided that reasonable assumptions concerning composition and roughness factor can be made. Vetter<sup>11/</sup> makes a somewhat similar calculation assuming that the layer is composed of  $\text{Fe}_2\text{O}_3$ . He uses  $5.3 \text{ \AA-cm}^2/\text{mc}$  to convert from charge to thickness. If in addition it is assumed that the roughness factor is unity when the current density is normalized to  $10 \mu\text{a/cm}^2$ , the thickness of the layer can be calculated. Under these assumptions the thickness of the

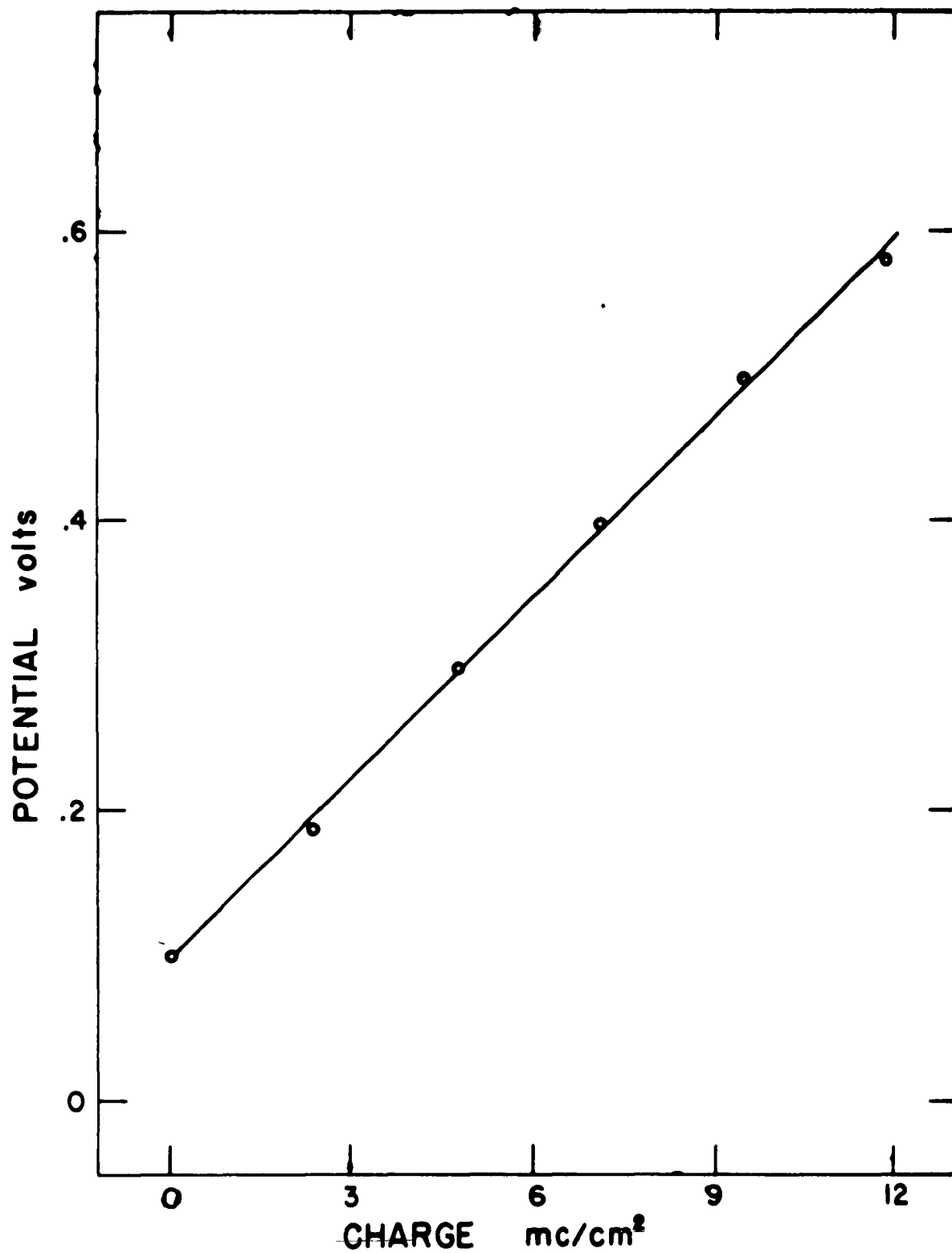


Fig. 27. Steady-state potential versus charge. Potential measured 100 seconds after switching down to steady-state current. Charge =  $(i - i_{ss})t$ .



layer is  $128 \text{ \AA/volt}$  expressed in terms of the steady-state overpotential. Expressed in terms of  $v_0$ , the thickness is  $331 \text{ \AA/volt}$ . The minimum thickness of the layer is then  $12.2 \text{ \AA}$ , and at an overpotential of .8 volts the thickness is  $102 \text{ \AA}$ . The jump distance associated with the barrier can be calculated if an assumption is made concerning the valence of the mobile charge carriers. Assuming that ferric ions are mobile, the jump distance is  $2.81 \text{ \AA}$ .

Fig. 16 showed, for anodic reduction, the dependence on passivating potential of the charge required to activate the electrode. When the slopes of Fig. 16 and Fig. 27 are compared it is seen that at an anodic current of  $3 \text{ \mu a/cm}^2$  approximately 30% of the layer is removed during the passive to active transition.

Many assumptions were required to arrive at the quantitative layer model described above. Until these assumptions receive some experimental support, the model must be considered as correct only to within an order of magnitude. While it is consistent with the simpler experimental results, it appears inadequate to explain the dependence of the overpotential parameters on current. Weil<sup>12/</sup> did not find this current dependence.

## VII. THE A-C IMPEDANCE

The a-c impedance measurements are taken as described in section II. The magnitude and phase angle of the a-c impedance are plotted against frequency in Fig. 28 and Fig. 29.

- The a-c impedance is well defined; it is independent of the amplitude of the signal for amplitudes up to at least 50 millivolts. The measurements plotted in Fig. 28 and Fig. 29 are taken at a passivating potential of .5 volts, but measurements taken at other potentials have essentially the same frequency dependence. To a zero order approximation the a-c impedance of the cell appears to be that of a capacitance.

The transient measurements show that the cell behaves as an exponential overpotential element in parallel with a capacitance. The electrolyte resistance appears in series with these parallel elements. For small a-c signals the exponential element can be considered to be a resistance,  $R$ , given by the equation:

$$R = (dv/di)_{i=i_{ss}} = v_o/i_{ss} \quad (11)$$

This equivalent circuit accounts for the general features of Fig. 28 and Fig. 29. Over the middle range of frequencies the capacitance dominates the a-c impedance. The decrease in the magnitude of the phase angle at low frequencies is due to  $R$ , and at high frequencies is due to the electrolyte resistance. For frequencies above  $10^5$  cps the impedance of the cell is approximately equal to the electrolyte resistance.

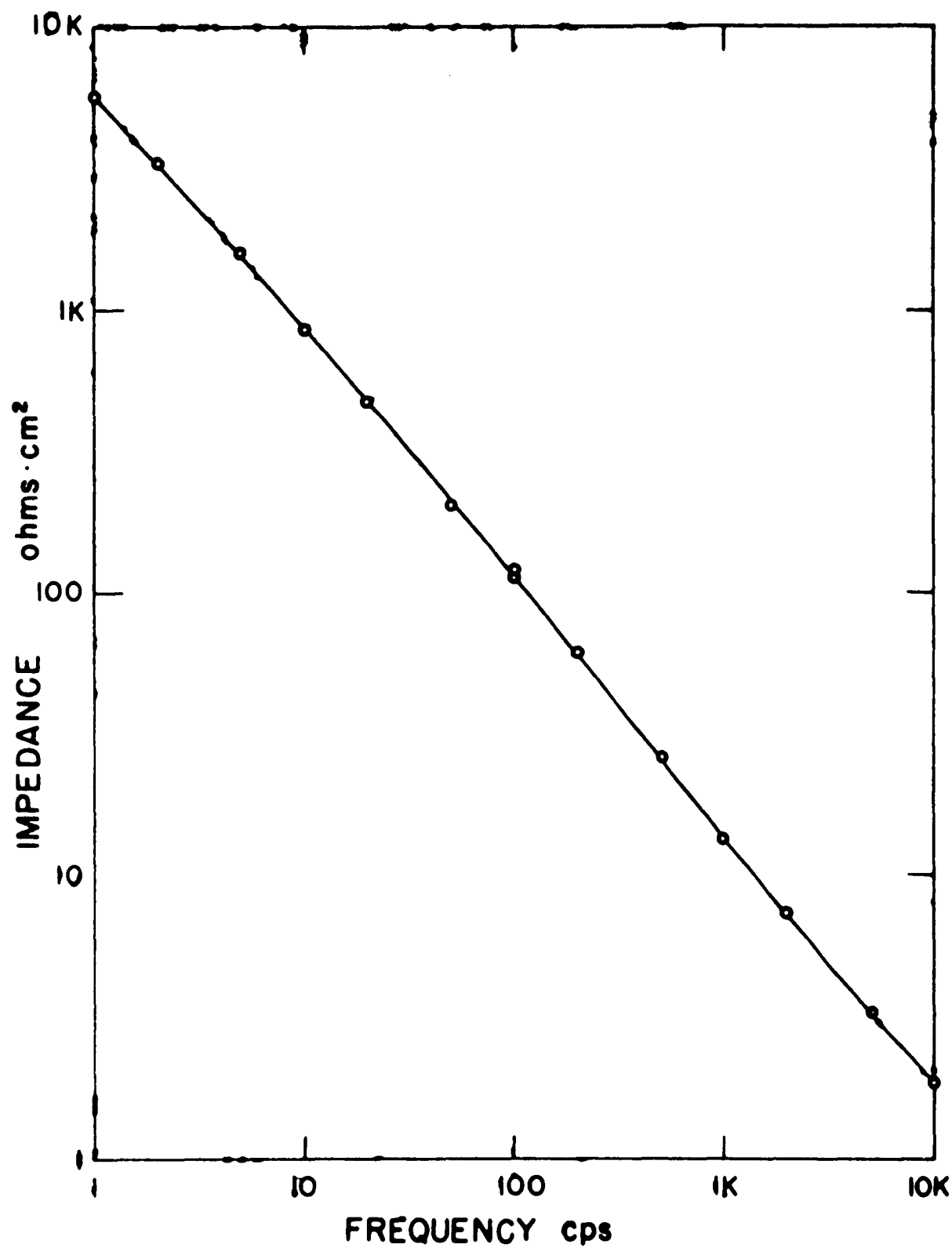


Fig. 10. Impedance versus frequency. Steady-state potential, 0.1 V.

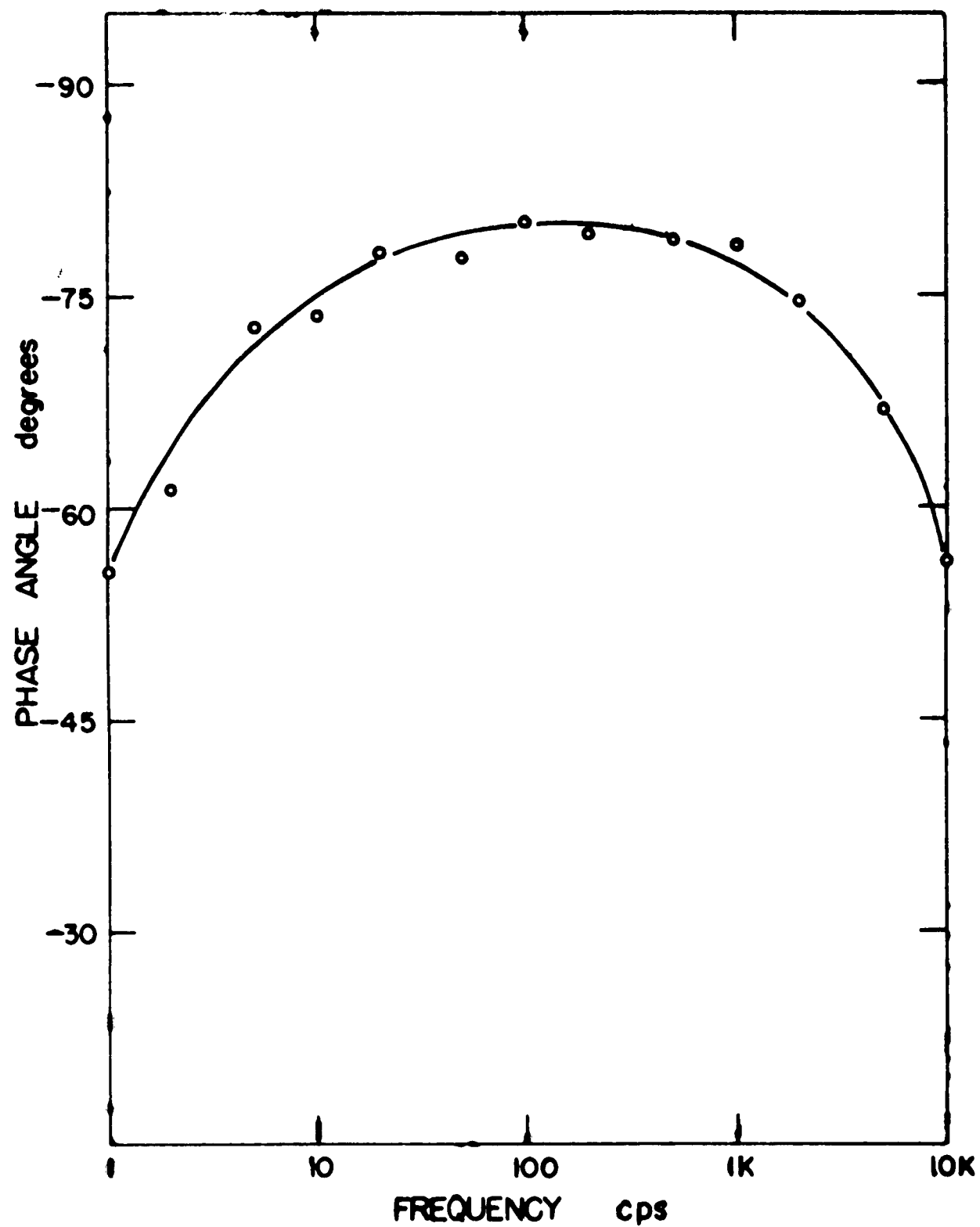


Fig. 29. Phase angle versus frequency. Steady-state potential, .5 volts.

The frequency range below 1 cps holds some interest, but the measurements are difficult to perform.

A slightly more general equivalent circuit is used for a quantitative study of the a-c impedance. The electrolyte resistance is calculated from the high frequency impedance, and is assumed independent of frequency and potential. The electrolyte resistance is subtracted from the resistive component of the a-c impedance. The remainder of the a-c impedance is represented by a resistance,  $R_p$ , and a capacitance,  $C_p$ , arranged in parallel. A comparison of the calculated values of  $R_p$  with Eq. (11) provides an indication of the extent of similarity between the transient and a-c behavior.

$R_p$  and  $C_p$  are plotted versus frequency in Fig. 30 and Fig. 31.  $R_p$  depends almost inversely upon frequency, especially at higher frequencies, changing by a factor of  $10^3$  as the frequency changes by a factor of  $10^4$ .  $C_p$  also depends upon frequency, but changes by only a factor of about two over the same frequency range. Eq. (11) makes no provision for a frequency dependence.

Fig. 32 and Fig. 33 show the dependence of  $R_p$  and  $C_p$  upon potential at a frequency of 100 cps. The reciprocal capacitance calculated from Fig. 33 was plotted in Fig. 13 along with the reciprocal capacitance determined from transient measurements. Some similarity is noted between the potential dependence of  $R_p$  and the potential dependence of the overshoot observed with galvanostatic thickening transients.

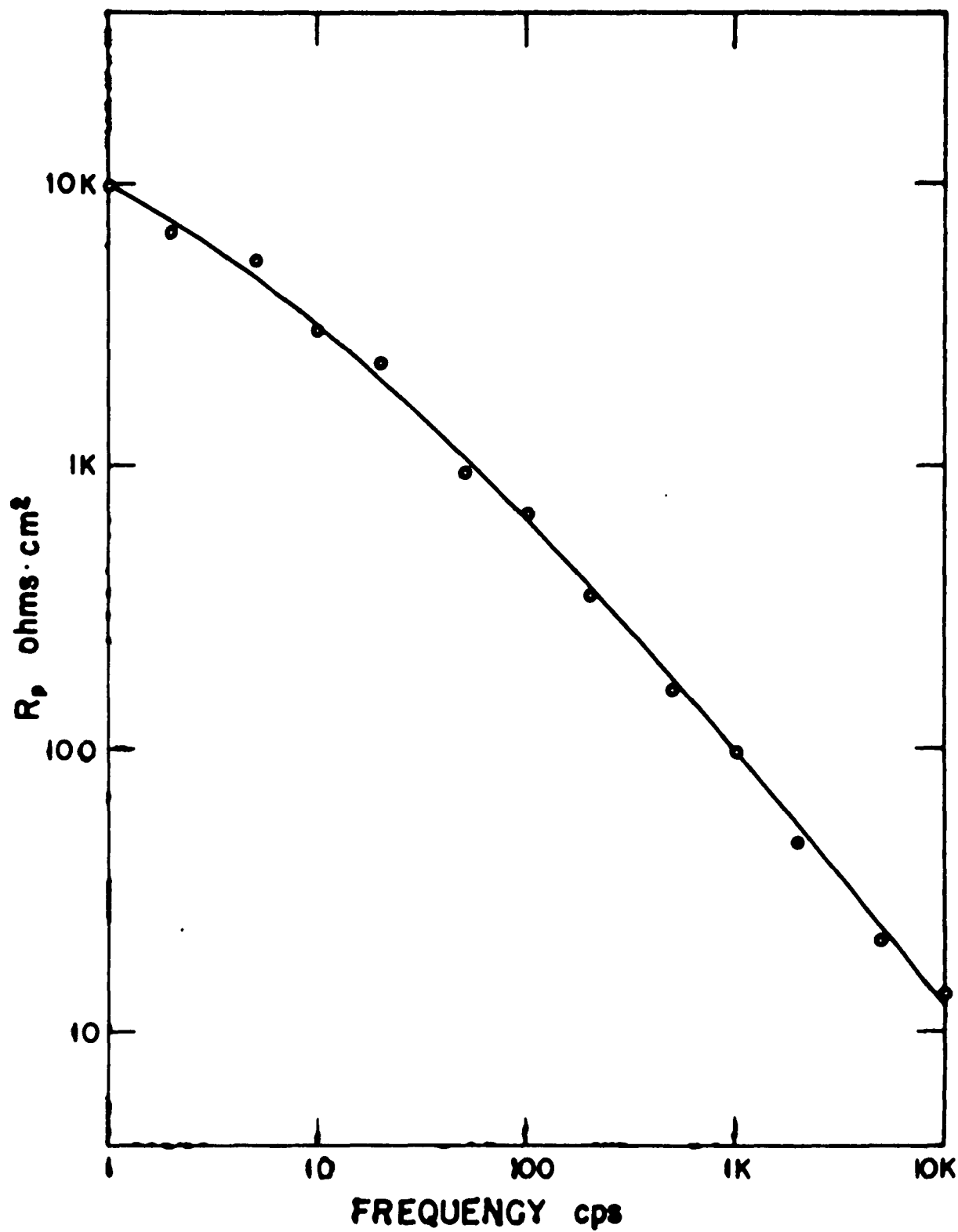


Fig. 30. Parallel resistance versus frequency. Steady-state potential, .5 volts.

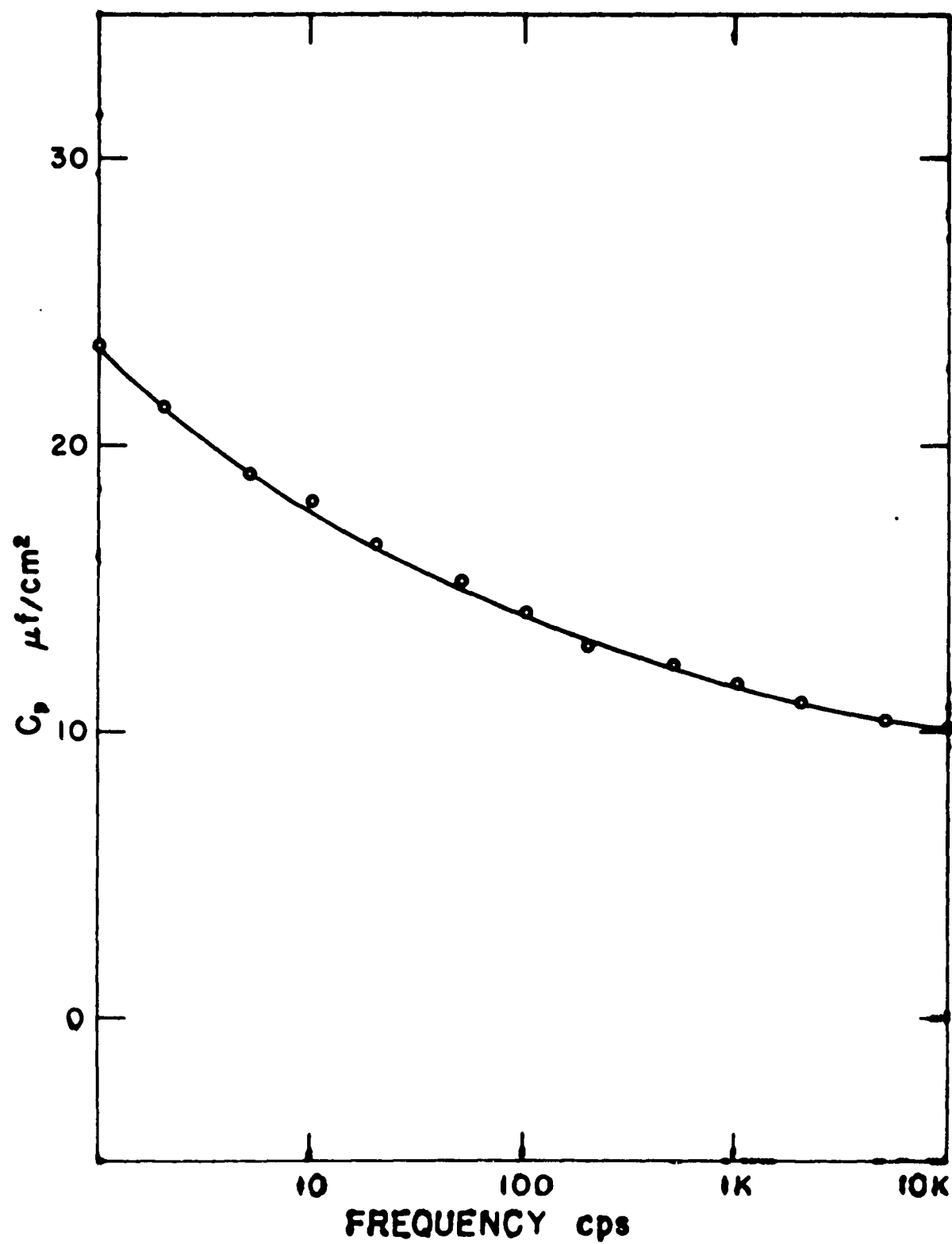


Fig. 31. Parallel capacitance versus frequency. Steady-state potential, .5 volts.

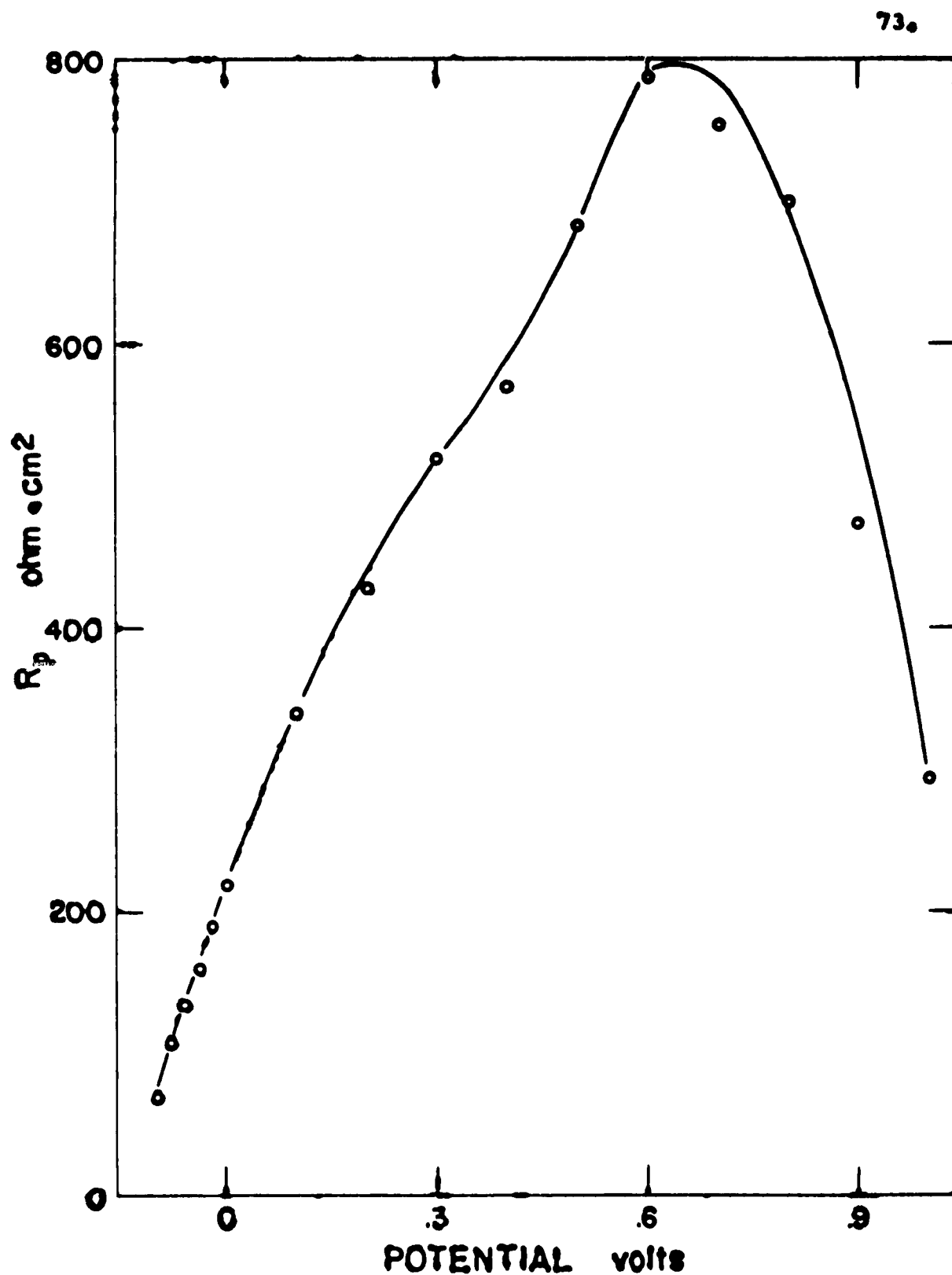


Fig. 32. Parallel resistance versus potential.  
Frequency, 100 cps.



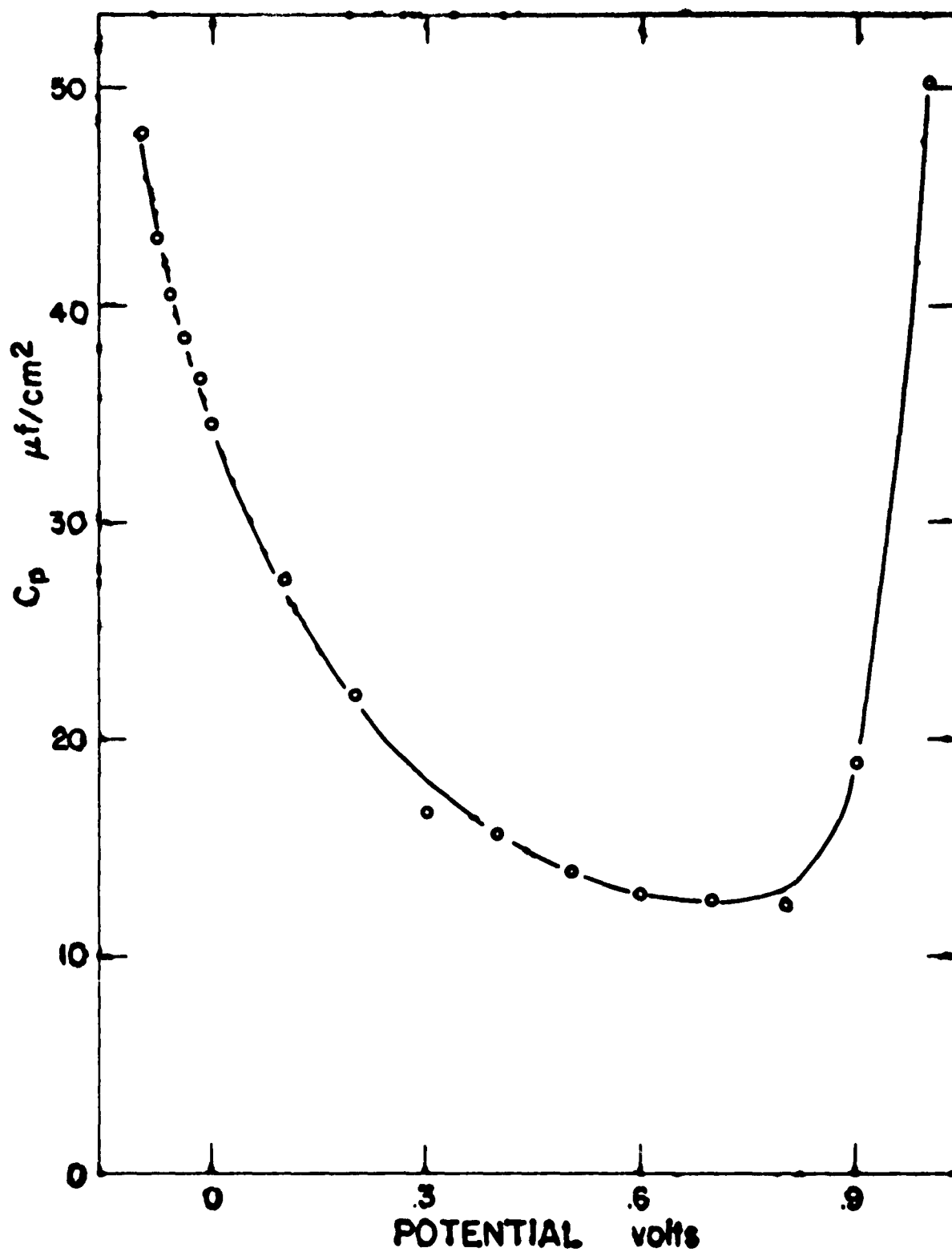


Fig. 33. Parallel capacitance versus potential.  
Frequency, 100 cps.

Other workers<sup>3,6/</sup> have obtained somewhat similar results, but arrive at rather indefinite interpretations. Engell and Ilschner<sup>6/</sup> use an equivalent circuit for a layer which is an electronic as well as ionic conductor to explain their transient measurements. The results derived by Grahame<sup>18/</sup> may be applicable to the a-c impedance of the passive iron electrode in spite of the additional complexity introduced by the presence of a surface layer. It is unlikely that a study of the a-c impedance will lead to an understanding of passivity; it is more likely that a complete understanding of passivity will be necessary before an explanation of the a-c impedance can be attempted.

## VIII. DISCUSSION.

All of the measurements described above are measurements of current or potential. Since the layer and adsorption theories of passivity attach different significance to the measured current, some discussion of this difference is given here. Layer theory assumes that the layer is dissolved in the acid at a constant rate dependent only on the acid concentration. This dissolution is assumed to require no net charge transfer between the anode and the electrolyte. The current passing through the cell is assumed to be associated with the layer formation reaction. The only effect the dissolution of the layer has upon the current is to determine the current at which a steady state is reached. The overpotential parameters are, under this assumption, associated only with the motion of charge carriers through the layer.

Adsorption theory assumes, on the other hand, that the observed current is the dissolution current. No adsorption theory in existence at the present time is as quantitative as the layer theory. Kolotyrkin<sup>13/</sup> states: "A definite condition of the metallic surface, characterized by a fixed overpotential for the anodic reaction, corresponds to each value of the potential lying in the passive region. If the surface is maintained in a given condition its speed of dissolution will vary with potential according to the usual Tafel straight line, just as in the case of an active, unpassivated surface."

Most of the experimental measurements of current and potential are interpreted in terms of the overpotential parameters  $v_0$  and  $i_0$ . A brief outline of the derivation of Eq. (5) will be given to bring out the physical significance of the overpotential parameters. Consider first a charged particle confronted by a potential barrier. The probability that the particle will surmount the barrier at any encounter is given by  $\exp(-U/kT)$ , where  $U$  is the height of the barrier and  $k$  is Boltzmann's constant. The number of particles crossing the barrier per second is obtained from this expression by multiplying by the number (or more properly the activity) of the particles and by their mean vibrational frequency. The vibrational frequency is commonly taken to be the ratio of the thermal energy to Planck's constant ( $kT/h$ ). The number of particles crossing the barrier in the reverse direction is given by a similar expression. The net flux across the barrier is given by the difference between these two expressions. The resulting expression for the current will only be valid if the activities of the initial and final states are independent of the magnitude of the particle flux across the barrier. When this condition is valid, the current is said to be activation controlled.

The charged particles on opposite sides of the barrier set up an electric field which alters the shape of the barrier. No net flux of particles across the barrier is observed when the product  $a_1 \exp(-U_1/kT)$  is equal to

$a_2 \exp(-U_2/kT)$ .  $U$  is the activation energy and  $a$  is the activity. The subscripts refer to the initial and final states. The potential at which zero net current is observed is known as the reversible potential. Overpotential,  $\eta$ , is measured from the reversible potential. The magnitude of the current crossing the barrier in each direction at the reversible potential is known as  $i_0$ , the exchange current.

The current across the barrier can be written conveniently in terms of the overpotential and exchange current:

$$i/i_0 = \exp(\alpha\lambda\eta/kT) - \exp(-(1-\alpha)\lambda\eta/kT) \quad (12)$$

where  $\alpha$  is the fraction of the overpotential aiding the forward current, and  $\lambda$  is the valence of the charge carriers. When the current is considerably greater than the exchange current, the second term can be dropped, and the equation becomes simply:

$$i = i_0 \exp(\alpha\lambda\eta/kT) \quad (13)$$

This equation is similar in form to Eq. (5). Eq. (5) is not put in the form of Eq. (13) because it is not assumed that the experimentally observed overpotential,  $v$ , is an overpotential across an activation barrier. If  $v$  is identified with  $\eta$  then

$$v_0 = kT/\alpha\lambda \quad (14)$$

and  $v_0$  must be a constant. If  $v$  is assumed to appear across a layer of thickness  $D$ , and if it is further assumed that the current through the layer is limited not by a layer resistance but by an activation barrier which must be surmounted before

charge carriers can enter the layer, then the potential which aids the forward current across the barrier is given by  $aE$ , where  $a$  is the jump distance associated with forward movement of particles across the barrier, and  $E$  is the electric field at the barrier. If it is assumed in the case of a thin layer that the effect of space charge within the layer can be ignored, then  $E = v/D$ . This assumption is made by Cabrera and Mott in their theory of oxidation<sup>14/</sup> for the case of thin layers. Under this assumption

$$v_0 = kTD/a\lambda \quad (15)$$

When Fig. 11, the plot of  $v_0$  versus passivating potential, is compared with Eq. (14) and Eq. (15), a variable thickness layer model of passivity is found to be a good first order approximation.

Dewald<sup>15/</sup> characterizes the layer by a barrier height and jump distance for entry to the layer, and a barrier height and jump distance for motion through the layer. He takes space charge into account and derives an expression relating current and potential. Dewald's equations fit the experimental results to a first order approximation as well as do equations derived by ignoring space charge, and they are no better to a second order approximation. More theoretical and experimental studies will be necessary before the role of space charge in passivity can be determined. A space charge theory may be able to explain the current

dependence of the overpotential parameters plotted in

• Fig. 24 and Fig. 25.

Many of the experimental results can be correlated adequately using a layer model of passivity. The dissolution rate of the electrode is independent of potential except at low potentials. In the steady state, the current through the layer will be, by continuity, independent of position and such as to balance the dissolution. Fig. 11 shows that, in the steady state, the thickness of the layer is proportional to the overpotential, and hence the electric field within the layer is constant. At low potentials the thickness of the layer does not decrease below  $12.2 \text{ \AA}$ . Once this thickness is reached, the dissolution rate of the electrode begins to rise. The layer may only partially cover the electrode at low potentials. A partial coverage region has been observed during the anodic oxidation of platinum.<sup>16,17/</sup>

The net result of transients involving appreciable charge transfer can be explained in terms of changes in thickness of the passive layer. The difference in the time constants of potentiostatic transients between transients in which the potential is switched up and transients in which the potential is switched down is adequately explained in terms of the exponential dependence of current on potential, and the linear dependence of the rate of change of thickness on current excess. The net result of a galvanostatic transient in which the current is raised above its steady-state value is to cause the thickness of the layer to increase

linearly with time. The constant of proportionality calibrates Fig. 11, and hence determines the jump distance. Galvanostatic transients with anodic currents lower than the steady-state value also involve a change of thickness with time.

Galvanostatic transients with cathodic or zero current reach the active state in a time short compared to the time required for the layer to reach zero thickness. For sufficiently large reduction currents the charge required to reach the active state is constant and equal to  $.06 \text{ mc/cm}^2$ . If this is multiplied by the assumed charge to thickness conversion factor, a thickness of  $.3 \text{ \AA}$  is obtained. This thickness corresponds to a fraction of a monolayer. Transient measurements taken during the transition show that this result is consistent with a layer model. The electrode retains some feature characteristic of the initial steady-state potential during the transition. The experimental results are all consistent with the assumption that a layer is present, but for cathodic currents, the electrode is activated by some mechanism other than thinning of the layer. If the electrode can be activated without removing the layer, it can be argued that the layer does not "cause" passivity. Weil<sup>12/</sup> postulates that, although the layer is present, a "hole" of some kind is created in the layer. This postulate is difficult to support in view of the fact that the process shows no thickness dependence. Adsorption theory, on the



other hand, assumes that the electrode becomes active due to the disruption of the monolayer (or fraction thereof) of adsorbed ions. The experimental results do not contradict this assumption. Three experimental facts appear important in this regard: a constant amount of charge is required; the overpotential associated with electrode activation appears more characteristic of a barrier than a layer; the transition can be reversed at almost any point by reapplying the steady-state current. The last result shows that no parallel path for currents of any appreciable magnitude can be available across the layer at any point along the passive to active transition, hence no "hole" of any significant size can be present.

Some of our experimental results are not easily reconcilable with the layer model described above. First, the capacitance is not inversely proportional to the layer thickness. Second, the dependence of the overpotential parameters on concentration does not fit a simple layer theory.

Let us first consider the dependence of the capacitance on thickness. (The capacitance is placed in parallel with the exponential current element in the model, so that if the overpotential appears across a layer, so must the capacitance). Attempts to explain the dependence have been made already<sup>6,17/</sup> but do not seem very satisfactory. The matter is not simple, because of the involved nature of the charge profile between

the electrode and the electrolyte. Besides the electrical double-layer at the layer-electrolyte interface, the layer on the electrode has charge on both its surfaces, and perhaps within, and the metal surface may be charged. The actual circuit elements are not all passive, and the charge layers interact. While the capacitance measurements do not fit readily into a layer model, they do not rule it out.

The manner in which the overpotential parameters respond to changes in the environment is still to be explained. The "metal environment" is changed most conveniently by giving the current a different value. Our knowledge of the resulting  $i_0$  and  $v_0$  response is still incomplete experimentally. When the "acid environment" is changed by increasing the concentration, we can expect increased dissolution of the layer, with eventual attainment of a new steady-state current to balance this. At the same time, we find that  $v/v_0$ , i.e., the average field across the layer, is (experimentally) independent of the concentration. Since  $\ln i = \ln i_0 + (v/v_0)$ , this means that the change in concentration brings about an eventual change in  $i_0$ , but the details of this adjustment are at present unknown.

A complete theory of passivity must await the formulation of a quantitative adsorption theory, and further studies on the possible effects of space charge within the layer.

## IX. SUMMARY

Over most of the passive region, in the steady state, the current is independent of potential. At higher potentials, oxygen evolution occurs, just as if no layer were present. (If a layer is present on the electrode surface it must be an electronic conductor, perhaps by way of a tunneling mechanism.) At the low end of the passive region, as the potential decreases, the current rises. The cause of this is at present unclear, but in any case, it indicates increased dissolution of the electrode. The dissolution reaction has an activation energy of 1.58 ev, and the rate depends markedly on the acid concentration.

From the shape of the open circuit decay, it is apparent that a capacitive element is associated with the layer. This capacitance is measured using galvanostatic initial slopes and a-c methods. The values obtained by both methods agree fairly well with each other, and the reciprocal capacitance is found to be linearly dependent on overpotential, but not proportional to it. The a-c impedance consists of the above capacitance in parallel with a resistive element. The frequency dependence of these elements is shown in Fig. 30 and Fig. 31. The a-c resistance has little in common with the parameters determined from the transient measurements.

When the overpotential decay is analyzed, it is found that the current through the parallel element depends exponentially on overpotential, and the parameters of this

dependence are determined. The zero of overpotential is set at  $-.055$  volts, and  $i_0$  is constant (except at low potentials) and is equal to  $.746 \mu\text{a}/\text{cm}^2$ .  $v_0$  varies linearly with overpotential over most of the passive region, the slope being  $.386$ . As the overpotential tends to zero,  $v_0$  becomes constant and equal to  $.037$  volts. This behavior suggests that a variable thickness layer is present, and that  $v_0$  is a measure of the thickness of this layer. Both the concentration and temperature dependence of the steady-state current are found to be represented in the  $i_0$  factor, and not to any great degree in  $v_0$ .

If, starting from the steady-state, we reduce cathodically with constant current  $i$ , we find an overpotential  $v$  for the plateau, where  $v = -v_0 \ln i + \text{constant}$ . This  $v_0$  is approximately independent of passivating potential and is not at all similar to the  $v_0$  for the anodic current. The charge required to activate the electrode is independent of both current and passivating potential for sufficiently high cathodic reduction currents. The magnitude of this charge is  $.06 \text{ mc}/\text{cm}^2$ . (For anodic reduction the charge is linearly dependent on the passivating potential.) Transients applied along the open-circuit plateau provide two additional pieces of information: throughout the transition the thickness of the layer does not change appreciably, and the transition can be reversed by reapplying the steady-state current even as late as one second before the sharp transition to the corrosion potential.

Experiments on layer formation show that the rate of change of layer thickness is proportional to the amount by which the applied current exceeds the steady-state current. Using this constant of proportionality and making certain assumptions about the nature of the layer and its roughness factor, the thickness of the layer is found to vary from a minimum of  $12.2 \text{ \AA}$ , to  $102 \text{ \AA}$  at an overpotential of 0.8 volts. From the constant of proportionality between  $v_0$  and thickness, and the additional assumption that the mobile charge carriers are trivalent, the jump distance is calculated to be  $2.81 \text{ \AA}$ . Under other than steady-state conditions, the overpotential parameters have a complicated dependence on current and potential, which is plotted in Fig. 24 and Fig. 25.

## REFERENCES

1. Proceedings of the International Colloquium on the Passivity of Metals, Z. Elektrochem. 62, 619-830 (1958).
2. H. G. Feller and H. H. Uhlig, J. Electrochem. Soc. 107, 864 (1960).
3. A. M. Sukhotin and K. M. Kartashova, J. Phys. Chem. (U.S.S.R.) 33, 562 (1959).
4. J. H. Bartlett and L. Stephenson, J. Electrochem. Soc. 99, 504 (1952).
5. U. F. Franck and K. G. Weil, Z. Elektrochem. 62, 378 (1958).
6. H. J. Engell and B. Ilshner, Z. Elektrochem. 59, 716 (1955).
7. K. J. Vetter and D. Berndt, Z. Elektrochem. 62, 378 (1958).
8. Ya. M. Kolotyrkin, Z. Elektrochem. 62, 664 (1958).
9. J. O'M. Bockris and E. C. Potter, J. Electrochem. Soc. 99, 169 (1952).
10. G. Okamoto, H. Kobayashi, M. Nagayama, and N. Sato, Z. Elektrochem. 62, 775 (1958).
11. K. J. Vetter, Z. Elektrochem. 62, 642 (1958).
12. K. G. Weil, Z. Elektrochem. 59, 711 (1955).
13. Ya. M. Kolotyrkin, J. Phys. Chem. (U.S.S.R.) 34, 534 (1960).
14. N. Cabrera and N. F. Mott, Repts. Progr. Phys. 12, 163 (1948-49).
15. J. F. Dewald, J. Electrochem. Soc. 102, 1 (1955).
16. J. Giner, Z. Elektrochem. 63, 386 (1959).

17. H. A. Laitinen and C. G. Enke, J. Electrochem. Soc. 107, 773 (1960).
18. D. C. Grahame, J. Electrochem. Soc. 99, 370C (1952).

#### ACKNOWLEDGEMENTS

The authors wish to express their appreciation to Mr. W. P. Perkins for his assistance both in performing the experiments and in analyzing the data. Thanks are also due to Mr. L. D. Ferguson for his investigations of capacitance and concentration dependence, to Mr. J. E. Orme for his help with the a-c measurements, and to Mr. P. O. Schemmel and Mr. W. H. Trester for their help with data analysis.



UNCLASSIFIED

UNCLASSIFIED